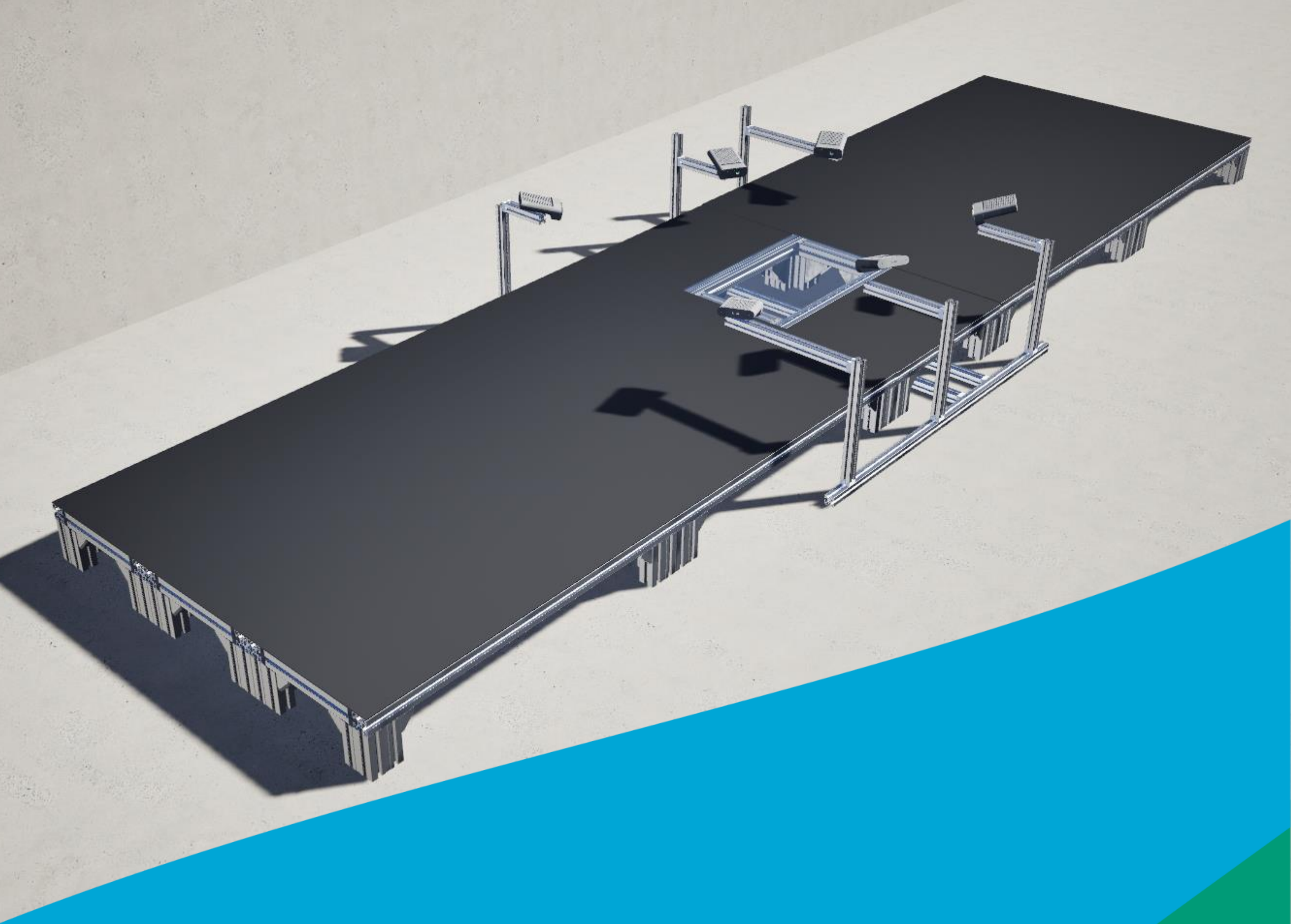

Dynamic Footprints

Redesigning 4D Scanning Hardware to Facilitate Natural Walking

Author: C.L.J. Eijck

Date: 28th of August

TU Delft

Dynamic Footprints

Redesigning 4D Scanning Hardware to Facilitate Natural Walking

By

C.L.J. Eijck

In partial fulfilment of the requirements for the degree of:

Master of Science
In Integrated Product Design
at the Delft University of Technology,
to be defended publicly on Friday, 28th of August, 2026, at 15:45

Thesis committee:	Chair:	Dr. Y. Song,	TU Delft
	Mentor:	Dr. T. Huysmans,	TU Delft

An electronic version of this thesis is available at http://repository.tudelft.nl/.

TU Delft

Preface & Acknowledgments

This thesis marks the completion of my Master's degree in Integrated Product Design at the Delft University of Technology. Although this project represents the culmination of my academic journey at TU Delft, it consistently challenged me to acquire new knowledge, proving that every project offers an opportunity to grow as a design engineer.

First and foremost, I would like to thank my supervisory team, Dr. Y. (Wolf) Song and Dr. T. (Toon) Huysmans, for their continuous guidance, support, and flexibility throughout a graduation process that followed anything but a conventional timeline. I am also very grateful to Farzam and Felix for their valuable technical insights and for answering my questions whenever I built upon their previous work.

Finally, I want to thank my family and friends for their unconditional support. Whether it was keeping me motivated when the going was tough, physically participating in any of the experiments, or helping me proofread this report, your support made all the difference.

Thank you,
Christiaan L.J. Eijck, Delft, August 2026

Contents

Abstract

The prescription of custom foot orthotics traditionally relies on static fitting methods, such as foam-box impressions or static 3D scanning. While these methods capture the foot's geometry in a single posture, they fail to account for the complex, dynamic deformations that occur during a human's natural gait cycle. Four-dimensional (4D) dynamic foot scanning addresses this by capturing the continuous 3D shape of the foot over time. This dynamic data has the potential to significantly improve the design and comfort of personalized footwear and orthotics.

To make this technology accessible, pioneering research at TU Delft previously developed a low-cost 4D foot scanner prototype (Vidmar, 2020; Kwa, 2021). However, an independent design evaluation of this prototype revealed critical mechanical and practical limitations that prevent routine clinical deployment. Most notably, mounting depth cameras directly onto the walkway frame left the sensors highly vulnerable to footstep-induced cadence vibrations. Furthermore, the system suffered from suboptimal sensor placement, camera resolution constraints, and a bulky, fixed structure that made it impossible to transport in a standard compact car, such as a Volkswagen Polo.

To overcome these barriers, this thesis focuses on the redesign of the 4D foot scanner to drastically enhance its technical reliability, clinical usability, and structural mobility. The proposed conceptual prototype features a modular, low-profile walkway design to improve patient accessibility and eliminate the fear of heights. To isolate the optical sensors from structural vibrations, a decoupled camera mounting system was engineered. Additionally, the bottom scanner was upgraded to Active Stereo Vision technology (Intel RealSense D405) with a shorter focal length to eliminate multipath interference from the glass plate and further lower the walkway height.

The physical dimensions of the redesign were rigorously evaluated through physical gait experiments and Virtual Reality (VR) simulation studies. The findings demonstrated that a 5-meter-long walkway is required to facilitate a truly natural gait pattern without the patient adjusting their stride, and that the combined effects of platform height and width significantly influence perceived patient discomfort.

Finally, optimal camera positioning was calculated to maximize view overlap, which successfully reduced the mean absolute scanning error from 3 mm to 2.25 mm. With a total component cost of €6.048,89, the physical prototype comfortably meets the financial requirements for low-cost clinical implementation. By solving the critical hardware and ergonomic challenges of previous iterations, this redesign provides a robust, mobile, and highly accurate foundation for the commercial adoption of 4D foot scanning in podiatry.

1 Introduction

1.1 Background and Clinical Context

In current clinical practice, podiatrists and orthopedic specialists rely heavily on static fitting methods to prescribe orthopedic aids, such as custom insoles. These traditional methods include foam-box impressions, pressure plates, goniometric angle assessments, and static 3D foot scans (Williams, 2020; Silva, 2024). While these conventional techniques effectively capture the anatomical geometry or pressure points of the foot at a single stationary instance, they fail to record the complex, dynamic deformations that occur across the full gait cycle (Tajdari et al., 2022; Kwa, 2021).

This static approach presents a significant clinical limitation. Conditions such as flat feet (*pes planus*), bunions (*hallux valgus*), and severe pressure-related injuries like diabetic foot ulcerations are highly dependent on the dynamic loading and biomechanical shifts that happen during walking. To address this limitation, four-dimensional (4D) dynamic foot scanning technology has emerged. This technology captures the continuous three-dimensional shape of the foot over time, producing a sequence of 3D meshes that effectively form a "video" of foot deformation during walking (Kwa, 2021; Thabet et al., 2014).

By combining 3D foot geometry with motion capture, a 4D scanner provides clinicians with crucial dynamic data, allowing them to quantify exact morphological changes such as dynamic arch collapse and toe splay. With these insights, podiatrists can design custom orthotics with precise dynamic allowances (e.g., specific arch-pad height tolerances or toe-box expansions), promising improved patient comfort, increased adherence, and the prevention of severe foot injuries in vulnerable patients (Barr, 2025; Boppana, 2021; Zhang, 2023). However, widespread clinical adoption by standard podiatry practices is currently hindered by significant barriers, including high equipment costs (€30,000 to €50,000+), space constraints in standard medical facilities, and the advanced technical expertise required for routine operation (Silva, 2024; Kwa, 2021; Thabet et al., 2014).

1.2 Technical Principles and Challenges

From a technical perspective, a 4D foot scanning system operates through an advanced multi-stage data processing pipeline. First, depth maps or images are synchronously captured from a distributed multi-camera network surrounding a specialised walkway platform. Every camera's position and orientation must be precisely calibrated, typically using checkerboard patterns, to align all views into a shared coordinate system (Shi, 2016; Barreto et al., 2022). Next, 3D point clouds are generated from each camera pair via stereo triangulation or direct depth computation. These point clouds are then registered into a common frame and refined using alignment algorithms like the Iterative Closest Point (ICP) method (Besl & McKay, 1992; Zhang, 2023). Finally, surface reconstruction algorithms—such as Delaunay triangulation, Poisson reconstruction, or marching cubes—are deployed to connect the points into a watertight mesh for each individual frame (Barreto et al., 2022; Solav et al., 2018), which must then be ordered sequentially in time and space (Hartley & Zisserman, 2004).

This dynamic approach introduces substantial engineering hurdles. High capture speeds (at least 30 frames per second) and resolution are critical to ensure high-fidelity scans without motion blur, resulting in massive data volumes that must be stored and processed (Kwa, 2021; Thabet et al., 2014). Furthermore, the physical impact of patients walking on the platform induces significant structural vibrations (Kwa, 2021). These vibrations disrupt the cameras' spatial alignment and lower scanning accuracy if left unmitigated. Cameras must also be meticulously positioned around the platform to maximise coverage and eliminate occlusion issues (Tajdari et al., 2022).

1.3 Problem Statement and Research Context

To bridge the gap between expensive commercial systems and clinical viability, previous research at TU Delft by Vidmar (2020) and Kwa (2021) focused on developing an accurate, low-cost 4D foot scanner prototype. While these pioneering prototypes successfully integrated 3D foot morphology with biomechanical data, an independent design evaluation reveals critical limitations that prevent routine clinical deployment.

Most notably, the previous iteration mounted the depth cameras directly onto the walkway frame, leaving the optical sensors highly vulnerable to footstep-induced cadence vibrations. In addition, the system is hindered by camera resolution constraints, suboptimal sensor placement and view overlap, user interface limitations, and gait acquisition bottlenecks. Beyond these technical challenges, portability presents a major obstacle. Field research requires a mobile device that can be transported to various locations and fit within a standard compact car, such as a Volkswagen Polo.

2 Assignment & Project Scope

2.1 The Challenge

The primary challenge of this graduation project is to redesign the previously developed 4D foot scanner prototype (based on the work of Vidmar and Kwa) into a reliable, user-friendly, and mobile device that is suitable for clinical implementation. An evaluation of the current prototype revealed critical limitations regarding reliability (walkway vibrations negatively affecting measurement accuracy), usability (complex manual camera alignment), patient interaction (anxiety and discomfort caused by the walkway's height and width), and mobility (the setup is too large and difficult to transport). This project focuses on solving these mechanical and hardware issues using commodity hardware to lower the barrier for routine clinical adoption.

2.2 Research Questions

To achieve this goal, the project addresses the following research questions:
How do the physical dimensions of the scanner (walkway length, height, and width) influence the comfort and natural gait pattern of the patient during a scan?
How can the camera system and its mounting be redesigned to fully isolate the sensors from step-induced structural vibrations?
What is the optimal camera positioning to maximize view overlap and eliminate blind spots, and how can the system facilitate a more intuitive camera alignment process?
How can the physical architecture of the scanner be made modular so that the entire disassembled setup fits into the trunk of a standard compact car (e.g., a Volkswagen Polo) to enable field research?

2.3 Expected Outcome

The expected outcome of this project is a physical, working conceptual prototype of the redesigned 4D foot scanner. This prototype will demonstrate the following optimized hardware elements:

- A walkway that does not impede in the natural gait of patients.
- Improved scan quality by changing key components of the system concerning the scanner.
- A decoupled scanner mounting system that is structurally independent of the walkway to prevent the transfer of footstep vibrations.
- A cost and physical analysis verifying that the hardware setup meets the financial and structural requirements for future clinical research (a cost of less than €30.000).

2.4 Out of Scope

Unlike the previous research by Vidmar and Kwa, which also focused heavily on embedded systems and data synchronization, the boundary of this project is strictly limited to hardware, ergonomics, and physical product design. The following aspects are explicitly out of scope:
Software development and integration: Because the new setup might utilize different camera ecosystems (such as the Intel RealSense D405 alongside the Azure Kinect), software integration becomes highly complex. Writing the software to synchronize or calibrate these systems is excluded from this project.
Data processing: Processing the raw scanning data via software into a usable 3D/4D model is also considered out of scope. Configuring the software settings or the user interface for the researcher is not part of this redesign.

2.5 Methodology

This project utilizes the 'Double Diamond' design methodology, consisting of alternating divergent and convergent phases: *Discover, Define, Develop*, and *Deliver*. A hybrid approach is applied: technical literature studies and sensor comparisons are combined with practical user research. This user research includes physical gait experiments and Virtual Reality (VR) simulation studies to iteratively test and validate human interactions with the device.

3 State of the Current 4D Scanner Prototype

To fully understand the technical and mechanical challenges of 4D foot scanning, it is essential to evaluate the current prototype developed by Vidmar (2020) and Kwa (2021). This chapter outlines the physical state of the scanner at the start of this project and highlights the specific hardware bottlenecks that prevent its routine clinical use.

3.1 The Physical Prototype

The current prototype consists of a wooden and aluminium walkway frame, equipped with a 60x60 cm transparent glass scanning plate. The system utilizes a multi-camera setup featuring Intel RealSense D435i depth sensors to capture the dynamic morphology of the foot from below and the sides. While this design successfully demonstrated the feasibility of low-cost 4D scanning, an independent design evaluation reveals several critical limitations.

Figure 1 - Current design of the scanner done by Kwa (2021)

3.2 Mechanical Evaluation

3.2.1 Camera Mounting and Vibration Isolation

In the previous iteration, the depth cameras are mounted directly onto the main frame of the walkway using narrow, 3D-printed plastic ball joints. This mounting solution is highly susceptible to mechanical 'creep' due to the continuous force applied by the cameras' weight. More importantly, because the cameras are physically coupled to the walkway, step-induced vibrations generated by the patient travel directly to the optical sensors. This structural interference significantly reduces the measurement accuracy and reliability of the device.

3.3 Optical and Technical Evaluation

3.3.1 Resolution and Framerate Constraints

The current Intel RealSense D435i setup operates at a framerate of 30 fps and a resolution of 848x480 pixels. Interviews with experts utilizing the scanner have revealed that this resolution is insufficient to achieve the sub-millimeter fidelity required for creating custom orthotic insoles. Any future scanner configuration must exceed these baseline parameters to ensure accurate 3D reconstructions.

3.3.2 Camera Positioning and View Overlap

Currently, the camera positions are exclusively focused on the center of the glass platform. However, there is no guarantee that a patient's foot naturally lands in this exact location. Furthermore, optimal 3D reconstruction requires maximum view overlap between the cameras, which the current alignment fails to prioritize. The alignment process itself is entirely manual and relies on a digital screen interface. Researchers have indicated that aligning the cameras is highly frustrating and imprecise, as the uniform background makes it difficult to visually identify which specific camera is being adjusted. This cumbersome calibration process further reduces the fidelity and usability of the scanner.

3.3.3 Focal Distance and Walkway Height

The focal length of the bottom scanner dictates the overall elevation of the walkway. The Intel RealSense D435i has a minimum focal distance of 28 cm, forcing the walkway platform to be elevated to approximately 30 cm. This height creates accessibility issues and subconscious discomfort for patients with mobility impairments. Reducing this focal distance is crucial to lowering the step-up height of the design and accommodating the clinical target group.

3.3.4 Synchronization and Interference

Due to the time-sensitive nature of 4D scanning, hardware synchronization between the distributed cameras is vital to prevent a distorted 3D capture. The current setup requires a DIY daisy-chain cable configuration and a custom trigger circuit, creating an unnecessary barrier for standard clinical implementation. While the Intel RealSense technology uniquely benefits from overlapping infrared patterns—which provide additional 3D landmarks to calculate the shape—the overall synchronization hardware remains a significant bottleneck.

3.4 Resulting Design Requirements

Based on the physical and technical evaluation of the current 4D scanner prototype, the following concrete design requirements are established to guide the redesign process:

- **Vibration Isolation:** The camera mounts must be structurally decoupled from the main walkway frame to ensure that step-induced cadence vibrations do not transfer to the optical sensors.
- **Resolution and Capture Speed:** The new scanning hardware must exceed the current baseline resolution of 848x480 pixels and maintain a minimum capture rate of 30 frames per second. This is required to prevent motion blur and provide the sub-millimeter fidelity necessary for orthotic design.
- **Intuitive Camera Alignment:** The system must accommodate a pre-calculated optimal camera placement to maximize view overlap. Furthermore, it must feature a mechanical alignment mechanism to replace the currently frustrating and imprecise digital calibration process.
- **Walkway Elevation and Focal Distance:** The chosen bottom scanner must have a minimum focal distance significantly shorter than the current 28 cm. This is essential to lower the overall step-up height of the walkway, thereby improving accessibility and comfort for mobility-impaired patients.
- **Hardware Synchronization:** The multi-camera system must offer a reliable, integrated hardware synchronization method, eliminating the need for complex DIY trigger circuits that hinder standard clinical implementation.

4 The Biomechanical Effects of Walking

The primary interaction patients have with the platform is walking. Walking is a dynamic process, which means the scanner has to handle different requirements than a static 3D scanner does. This chapter discusses the biomechanics of the gait cycle and the forces involved, and how these translate into physical requirements for the hardware.
Transitioning from static to dynamic 3D scanning introduces specific challenges related to ground reaction forces and the strict timing required to capture a moving patient, for example. Since gait and impact forces vary from person to person, these underlying biomechanical principles are further detailed below.

4.1 Gait cycle

Humans walk in a set pattern of steps, known as the gait cycle. Although this differs from person to person, the average cycle follows the stages shown in Figure 2. For this project, the most important part to capture is the window between the initial heel strike and the pre-swing phase.

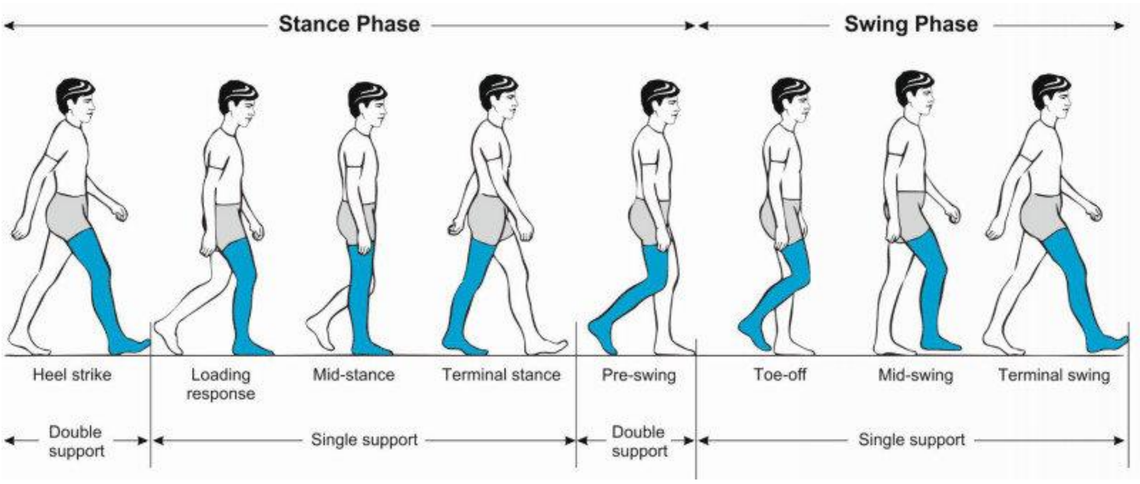

Figure 2 - Gait cycle during walking (Çağatay, Emre, & Seda, 2022)

This part of the cycle is important because it is when the foot undergoes the most deformation. By capturing this 'dynamic morphology' during movement, the scanner provides more useful data for clinicians than a static scan could (Vidmar, 2020; Kwa, 2021). However, capturing this movement accurately requires the right timing and space.

4.2 Step length

Capturing a natural, unforced gait cycle at this speed means the patient needs enough room to accelerate to their normal pace and safely decelerate afterwards.
The average step length is approximately 71 cm. This number is influenced by factors such as age, stature and sex (Mobbs, et al., 2025).
In the current design, that means the patient reaches the scan point in 2 steps. This is a potential issue since the patient might not be able to reach their normal gait or might already have altered their normal gait due to the short distance. To verify if this has an effect and in which way a study is done in chapter 6 and 7.

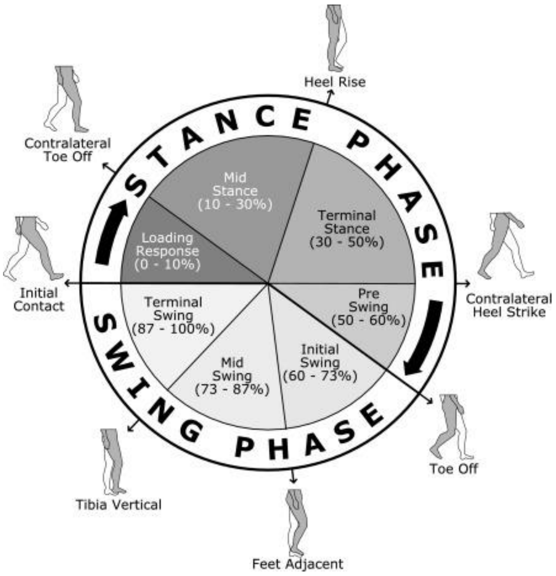

Figure 3 - Time spent in each phase (Arnaldo & Anselmo, 2022,)

4.3 Step time

Using the study by Mobbs et al. (2025), it can be calculated that the gait cycle lasts between 1.01 and 1.16 seconds. According to Root et al. (1977, as cited in Kwa, 2021), only 62% of that time is spent in the stance phase that needs to be captured, which gives a time frame between 626 ms and 719 ms to capture all relevant data.
Certain phases only last 10% of the total time, meaning a frame needs to be captured at least every 100 ms, which gives a minimum speed criterion of 10 fps for the scanner. In practice, this would probably be insufficient due to the fast-paced changes in the morphology of the foot.

Vidmar's (2020) prototype used a capture rate of 15 frames per second. This speed only produced 8 to 9 usable frames during the entire stance phase. This was not sufficient for a detailed motion analysis and increased the risk of motion blur. Kwa (2021) confirmed this limitation and determined that the framerate needs to be at least 30 fps to capture usable frames to create a fluent 4D scan. This sets a firm design criterion of 30 fps for the scanner.

4.4 Ground Reaction Forces

Walking generates ground reaction forces (GRF) that significantly exceed a person's static weight. Kwa (2021) previously modelled these dynamic loads for a 300 kg patient using a 33% safety margin. This resulted in a peak load requirement of 4000 N for the glass plate, which was used to validate the glass thickness required to prevent optical distortion. Consequently, the glass specifications from this previous iteration are adopted directly.
However, the currently proposed 200 kg patient was only accounted for in a static situation in the previous design by Kwa (2021). In reality, these forces are dynamic. During regular gait, vertical reactive forces peak at 1.3 times the body weight (Winter, 2009). For a 200 kg patient (2000 N static load), g=10 was chosen to have an additional safety margin, which is important in medical devices. This dynamic effect results in a force of 2600 N during normal walking. To ensure patient safety, a safety factor of 2 is applied to this dynamic force, establishing a final vertical design load of 5200 N.
Regarding lateral and longitudinal forces in the *xy*-plane, literature indicates that a force of 0.2 times the body weight is applied in the forward direction immediately after heel strike (Winter, 2009). This assumption is based on the walking gait of a healthy subject. To compensate, the platform must provide an equal braking force in the opposite direction. For a 200 kg patient, this equates to 400 N. Applying the identical safety factor of 2 yields a total horizontal design load of 800 N.

4.5 Potential research avenues

As mentioned above, the current length of the walkway limits the user to only two steps to the scan area. Because this restricted distance might force an unnatural gait cycle and thereby affect the validity of the gathered data, a study of its influence has been done in chapter 5 and 6. This needs to be done to come to a suitable measurement for the final length of the walkway.

4.6 Resulting Design Requirements from a biomechanical perspective

To ensure the successful development of the redesigned 4D scanner, the biomechanical constraints discussed in the previous sections must be translated into concrete hardware requirements. These parameters will serve as the foundational boundaries for the physical design and its structural validation.

- **Capture Speed (Framerate):** The optical system must operate at a minimum capture rate of 30 frames per second (fps). Since specific phases of the gait cycle can last only 100 milliseconds, this speed is crucial to capture the dynamic morphology of the foot with high fidelity and without introducing motion blur.
- **Vertical Load Resistance:** The underlying frame, connectors, and transparent scanning plate must be engineered to withstand a peak dynamic point load of 5200 N in the Z-direction. This requirement accounts for a 200 kg patient generating ground reaction forces up to 1.3 times their body weight during normal walking, combined with a mandatory safety factor of 2.0 to ensure patient safety.
- **Lateral Load Resistance:** The structure must be sufficiently rigid to resist lateral forces of up to 800 N in the XY-plane. This lateral force is generated during the heel strike phase; the frame must not shift or vibrate under this load, as any movement would directly disrupt the precise calibration of the cameras.
- **Unrestricted Movement:** The physical dimensions of the walkway must provide the patient with sufficient uninterrupted space. The approach and exit length must be long enough to accommodate natural acceleration and safe deceleration, ensuring that the captured gait cycle is unforced and clinically valid

5 User Journey

An analysis of the user journey was done. This analysis can identify potential design opportunities and allow one to understand the interaction with the scanner. This analysis is done from two perspectives: the researcher operating the device and the patient being scanned. Understanding these workflows helps to define the practical requirements for the redesign. This analysis was conducted through a role-playing cognitive walkthrough, utilizing the existing physical prototype developed by Kwa (2021) to simulate the experience of both the researcher and the patient.

5.1 The researcher

In Figure 4 below, an analysis of the interactions of the current design from the researcher's perspective is visualised.

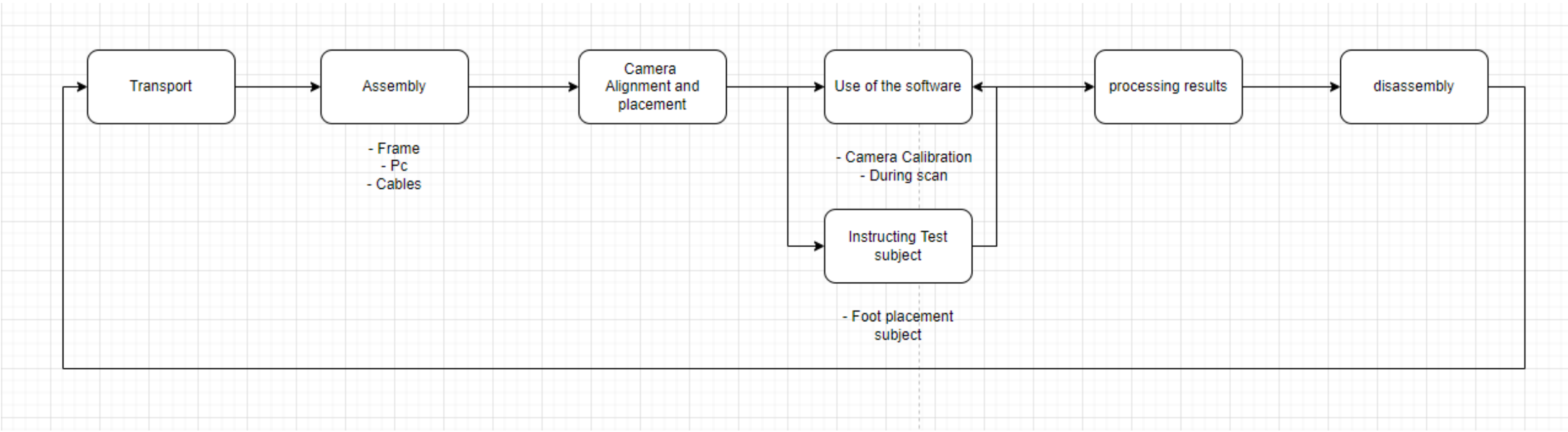

Figure 4: Storyboard of research interaction with the scanner

The researcher needs to be able to transport the scanner due to the fact that scanning happens at various locations. Therefore, an important requirement is that the disassembled frame fits within the trunk of a compact car, such as a Volkswagen Polo.
When the researcher arrives at the location, the researcher has to assemble the frame, manage the cables for safety, and connect and set up the computer.
The most important step in this setup is placing and aligning the depth cameras. Kwa (2021) emphasises that precise camera calibration and positioning are important to minimise calibration errors. If the alignment is incorrect, the precision of the 3D data decreases significantly. Hence, an intuitive and reliable alignment mechanism is an interesting design opportunity for the new design.
After the physical setup, the software is prepared, and the patient is instructed. After the patient has walked across the scanner, the scanning session is over, the walkway needs to be cleaned to meet hygienic standards, and the scanner is disassembled for transport. The software processing happens afterwards and is considered out of the scope of this project.

5.1.1 Requirements for the design from the researcher's perspective

From this workflow, several design opportunities are found:
Portability: The largest parts must fit in the trunk of a compact car. To make it a concrete requirement, the longest part may not exceed 1m.
Assembly: A modular system is needed for quick assembly and disassembly without specialised tools. Additionally, the fewer components required, the faster the setup can be deployed.
Cable Management: A solution to route the cables and prevent tripping hazards.

Camera Alignment: A mechanism to ensure the cameras are positioned correctly for calibration (Kwa, 2021).
Patient Positioning: A way to help the researcher quickly guide the patient's foot placement.
Hygienic Maintenance: The materials used for the walkway surfaces must be resistant to cleaning agents.

5.2 The patient

Any patients that needs to be scanned also have an interaction with the scanner. This interaction is different from the researcher's since the use differs. In Figure 5, the rough timeline of the interaction can be seen.

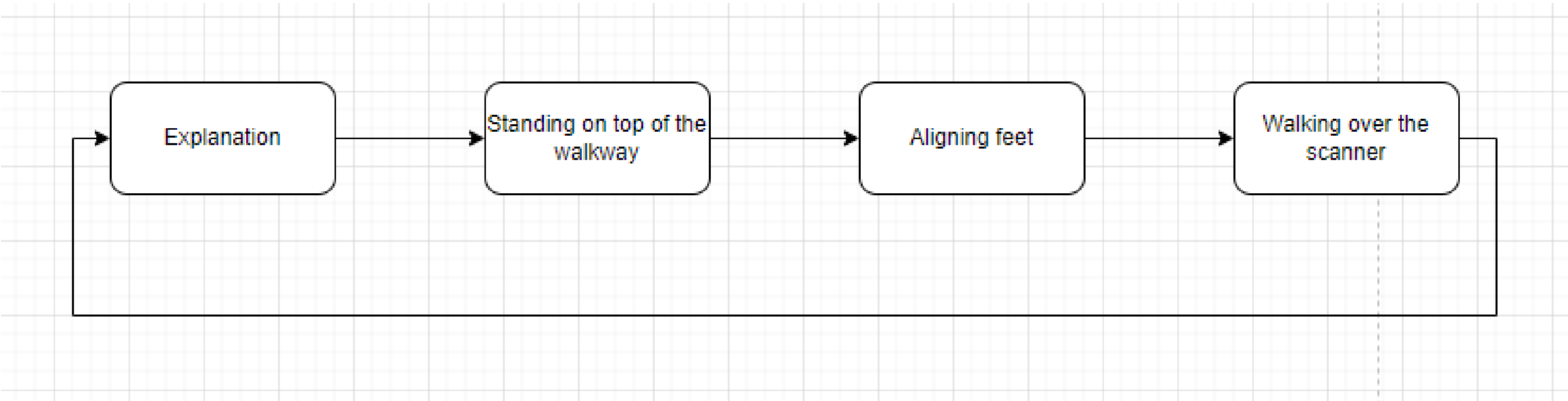

Figure 5: Storyboard of patient interaction with the scanner

First, the researcher explains the process to the patient. Afterwards, the patients need to remove their shoes and socks to allow the foot to be scanned as well as to prevent damage to the glass plate. Then the patient can step on the walkway.
When on the scanner, the patient experiences the textures of the walkway with his foot. After the researcher gives the instruction, the patient walks across the scanning area. To get a complete 4D model of the gait cycle, this walking process often needs to be repeated multiple times (Vidmar, 2020).

Since the target group for orthopaedic research often entails elderly people or patients with mobility issues, safety and comfort while stepping onto and walking across the scanner are crucial design requirements and offer interesting design opportunities.

5.2.1 Requirements for the design from the patient's perspective

Based on the patient's perspective, the following points provide interesting design opportunities:

- **Accessibility:** A safe and easy way to step onto the elevated walkway, especially for patients with mobility issues.
- **Fall Prevention:** a method to ensure patients do not step off the edge, lose balance, or slip.
- **Walkway Guidance:** a way to indicate to the patient where to start and end their scan
- **Walkway Length:** The walkway must be long enough to capture a natural gait cycle.
- **Comfort:** The surface texture needs to be comfortable for bare feet while providing enough grip to prevent slipping.

6 Camera Placement

To achieve the sub-millimeter fidelity required for custom orthotics, the multi-camera system must be precisely aligned to maximize view overlap and eliminate blind spots. The current scanner configuration relies on the assumption that a patient will naturally place their foot in the exact center of the scanning plate. However, in clinical practice, a natural variance in the heel strike location is inevitable due to individual differences in body proportions and gait patterns. If a patient's foot lands outside the optimal focal area of the cameras, the quality of the 3D reconstruction degrades significantly.
To ensure the newly designed scanner can accommodate this human variance without losing accuracy, it is crucial to understand where patients naturally step. Therefore, an experiment was conducted to map these foot placement patterns and to investigate whether giving patients a predetermined starting position can reliably guide their final heel strike to the center of the scanning area. The spatial data acquired from this experiment will directly serve as the foundation to calculate the optimal, mathematical camera coordinates for the redesigned scanner. *(The full methodology and execution of this experiment can be found in Appendix: Aligning participants' steps with the scan area experiment 1).*

6.1 Foot placement experiment

To accurately map natural foot placement patterns and test the effectiveness of visual starting guides, a physical walking experiment was designed.

6.1.1 Method

The experiment was done with 8 participants (3 females and 5 males), 6 within the age range of 20 and 30, 2 around 60 years, with varying heights between 1.6m and 2.1m and BMI between 21 and 28.7.
Three runs were done with different commands.
During one walk, the participants were instructed to place their foot in the middle of a drawn box.
For the next walk, the participants were instructed to place their feet in a certain position from the edge and were given the command to walk to the other side from the appointed start position.
This formula was as follows;

$$Steps\ to\ the\ middle\ of\ the\ platform\ =\ Distance\ to\ the\ half\ of\ the\ platform\ /\ Steplength$$

The number that follows is almost always a whole number with some decimals.

$$\text{Distance to compensate} = \text{decimals} * \text{steplength}$$

The result of this calculation gives the distance to compensate so the heel strike is in the middle of the platform.

The last option was for the participant to walk normally to the other side.
To capture the location of the heel strike of each participant, paint was applied to their feet, and they were instructed to walk across in several different manners to see if it is possible to reduce the variance of the location of the heel strike while ascertaining a natural walk.

6.1.2 Results

Figure 6 - Example of 1 participant walking down on the paper

The resulting painting was digitally overlaid to show where the average foot location of each participant depended on the assignment given.
The results can be seen in Figure 7 and Figure 8.

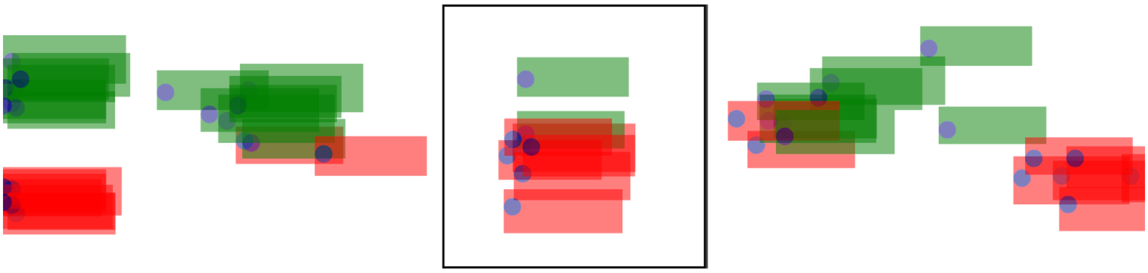

Figure 7 - Participants were instructed to try to land their feet in the middle without further instructions (red = right foot, green = left foot, blue dot = heel strike)

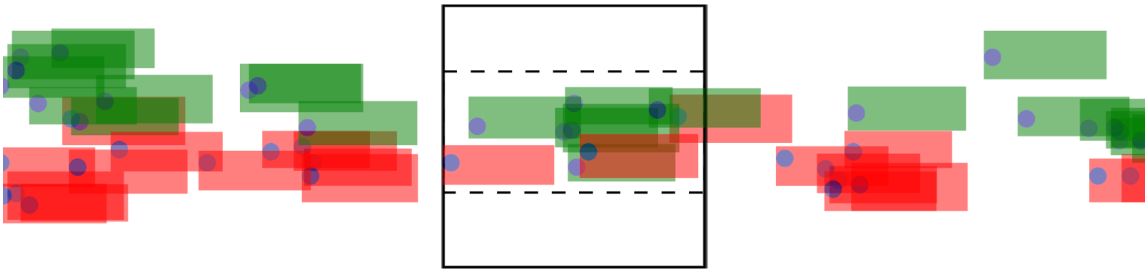

Figure 8 - Participants were instructed where to place their feet and to walk to the other side (red = right foot, green = left foot, blue dot = heel strike)

It was found that people, with the proper instruction and foot placement, were able to land their feet naturally in the same area. The area is shown in Figure 9 below.

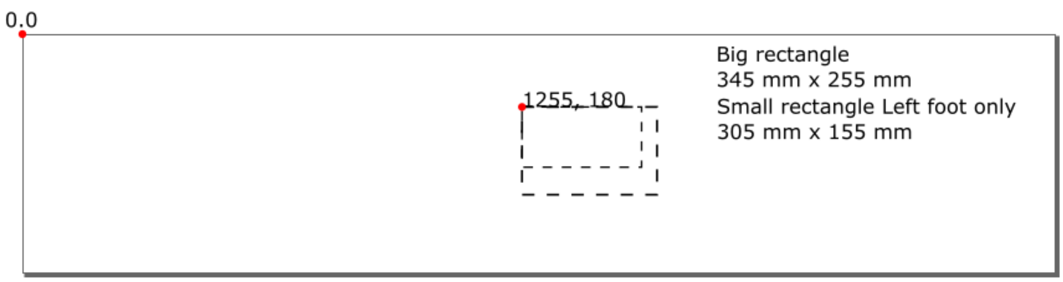

Figure 9 - Average foot position of participants

Figure 9 shows the bounding box that was used to calculate the right positioning for the camera.

For the height, one participant was measured while standing on their toes to the middle of their ankle joint. This resulted in a distance of 17 cm.

6.1.3 Conclusions

Foot placement

When comparing methods 2 and 3, it can be seen that just instructing the participants to place their feet in the middle of the square does not allow for a natural walk. This can be seen in that the participant already struggles to think about which foot to start and during their walk kept looking down. As well as their step size, where the step that lands in the middle of the platform is bigger than usual.
When the starting position of the feet was given, a more natural walking pattern emerged. The participant walked without looking down, and the step sizes were more consistent.

Formula

It was found that the current formula did not account for the length of the foot so the last part of the
The formula needs to be changed to;

$$Distance\ to\ compensate = decimals * steplength * 0.5 * footlength$$

This would ensure the foot lands in the middle of the walkway.

Placing the foot in the calculated Position

Placing the foot upon the calculated position was cumbersome for the participant as well as the researcher. The spot where the foot needed to be placed needed to be marked and measured with tape measures. This process could be eased by using a grid-like system where it is visible where the foot needs to be placed

Length of the walkway

The current length of the walkway up to the scanner is not sufficient. The step size of most participants was still increasing, and for people with a bigger step size >70cm, the walkway is too short, it was observed during the experiment and confirmed by questioning after that the participants would reduce their final step to stay within the confines of the paper walkway.
To ensure all participants would have set 3 steps at least before placing their 4th footstep on the scanner, the walkway needs to be 2.85 cm long. To verify if this is needed, further studies need to be done.

6.2 Calculated Optimal Position of the Cameras

In a recent study, the optimal positions for all the cameras were calculated using data acquired from the experiment. Farzam Tajdari assisted with this calculation, which involved inputting several parameters about the cameras and the bounding boxes of the feet. It was stipulated that cameras could not be placed above the walkway. The results of the calculation are depicted in
Figure 10 demonstrates an optimal setup for the cameras.

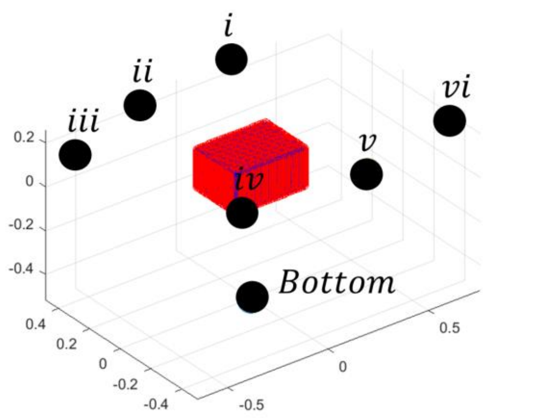

Figure 10: Camera placement in 3d dimensional space

Table 1 shows the optimal coordinates for the specific set-up that is illustrated above.

Table 1 - Camera Coordinates in cm for optimal Intel RealSense Set-up

	Cam 1	***Cam 2***	***Cam 3***	***Cam 4***	***Cam 5***	***Cam 6***	***Bottom***
X	28	-22	-65	-55	25	63	0
Y	48	43	30	-50	-43	-30	0
Z	26	25	23	26	17	17	-45

After this, both cameras were set up in the original orientation and the optimal set-up. With each camera, a photo was taken.
These photos were processed into a complete model with the help of a non-rigid ICP model. The complete 3d model of each set-up was compared to a scan of the object that was made by the Arctic Eva. This scan was used as a baseline due to the high accuracy of the scan from the Arctic Eva.
The difference in accuracy due to the new set-up is visualised in Figure 11 and Figure 12.

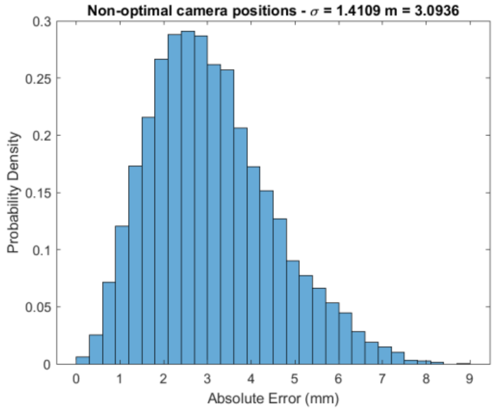

Figure 11 - Non-optimal camera position

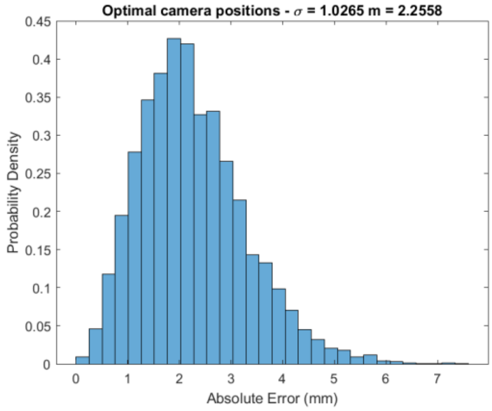

Figure 12 - Optimal camera position

As is seen in the graphs, the optimal set-up reduces the mean error from 3mm to 2.25mm. This means the accuracy overall of the scanner is improved by 0.75mm.
This difference was only due to the change in position and not in the cameras.
The standard deviation was also reduced. This means the scan was better at following the topology of the surface of the scanned object.

The assumption is that the accuracy will further improve when the change is made to a better scanner.

6.3 Resulting Design Requirements from the foot placement study

- **Application of optimal camera positioning:** As demonstrated, camera positioning has a significant influence on the final fidelity of the scan. Therefore, it is essential to apply this calculated setup directly to the final scanner configuration.
- **Algorithm recalibration for hardware changes:** If any changes are made to the scanner hardware or camera specifications in future iterations, this positioning algorithm must be run again to recalculate the optimal angles and distances.
- **Impact of physical constraints on natural gait:** The physical constraints of the current setup actively force participants to alter their natural gait cycle. This directly compromises the primary clinical goal of the 4D scanner, which is to capture an uncompromised, natural walking pattern.
- **User compensation behavior:** It was observed that individuals actively reduced their final step length to stay within the restricted confines of the current platform.
- **Necessity for systematic follow-up research:** To resolve this issue, follow-up research is crucial to systematically quantify exactly how the physical dimensions of the design—specifically the length, height, and width of the walkway—affect a patient's stride and perceived discomfort.

Transition to the next chapter: The following chapter (*Chapter7: Dimensional influences of the design on the gait of the patient*) will systematically investigate these dimensional influences to establish the optimal physical requirements for the redesigned walkway

7 Dimensional influences of the design on the gait of the patient

As observed during the initial foot placement experiments (6.1.3), the physical constraints of the current setup actively force participants to alter their natural walking pattern. Most notably, individuals subconsciously reduced their final step length to stay within the restricted confines of the short platform. However, beyond just the length, the perceived safety of the walkway—dictated by its height and width—can also induce subconscious discomfort or a fear of falling, which further skews the biomechanical validity of the scan.
Because capturing an uncompromised, natural gait cycle is the primary clinical objective of this 4D foot scanner, these structural dimensions cannot be arbitrary. Therefore, this chapter systematically quantifies exactly how the length, height, and width of the walkway influence a patient's stride and perceived distress. The outcomes of these subsequent experiments will directly establish the fundamental physical requirements for the redesigned walkway.

7.1 Influence of the gait due to the length of the walkway

From the previous experiment, several questions arose regarding the potential impact of walkway length on individuals' step lengths and, subsequently, on the accuracy of the scans for natural walking gaits. To investigate these effects, the following hypotheses were formulated:

From the previous experiment, it was observed that participants would reduce their final step length to stay on the walkway when reaching its end. This change in step length could indicate a change in the walking gait as a whole, and this needs to be prevented if the goal is to capture the natural gait of an individual. To see if the walkway length affects the step length, the following hypothesis was formulated:

1. Due to the short length of the 3-meter walkway, it is expected to influence an individual's step lengths significantly.

Furthermore, in the previous experiment, the step length seemed to increase due to repeated walking on the same walkway. This effect could influence the results of a scan and would need to be accounted for if these scans are used to design inserts. To verify if this assumption was happening, the following hypothesis was formulated:

2. Step length increases after repeated use of the walkway.

The current design of the scanner features a glass plate of 60*60 cm. For a potential redesign, it was hypothesised that a smaller scan plate might make it easier for patients to align their feet to the middle of the plate.

3. The width of the glass plate is expected to have an impact on the proximity of participants' steps to the middle of the scan plate.

To systematically quantify how the physical length of the walkway alters a patient's natural stride, an experimental setup using a Gaitrite measurement mat was deployed.

7.1.1 Method

To systematically evaluate how different walkway lengths affect a patient's natural stride, a physical walking experiment utilizing a Gaitrite measurement mat was conducted. The full study and its detailed procedure can be found in *Appendix: Aligning participants' steps with the scan area experiment 2*.
General information about the 17 participants was gathered. These details included age, weight, height, and the dominant foot. The ages ranged between 18 and 65, and the length ranged between 1,5m and 2,10m. Each participant was asked to complete multiple runs on the walkway where the length varied between 3m, 5m, and unobstructed.
For each length, an unobstructed run was done to set a baseline step length for each length. Afterwards, they were asked to target the centre of a red cloth, which represented the scan plate, for each length. The cloth could be in a smaller size (60x45cm) or a bigger size (60x60cm) to simulate the change in dimension of the glass plate. The order of length and cloth size was randomised to minimise potential carryover effects.

7.1.2 Results

Data were collected from a total of 17 participants, each of whom completed three runs for each test, resulting in a substantial dataset. An example of the results, which have been converted to a plot, can be found in Figure 13. The right side is the starting point of the walkway, and where they step over the box can be seen in the plot by where they feet are planted next to another around the 3m mark. As can also be observed from the plot, the Gaitrite measured the distance from 600 to 0.

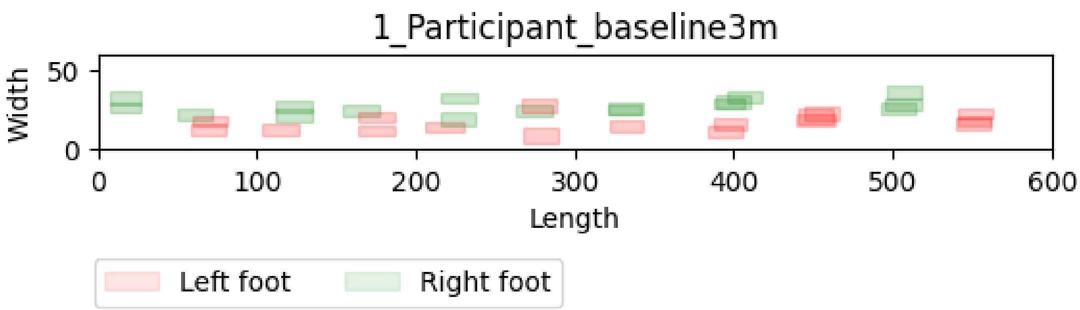

Figure 13 - Example of the final data collected and converted into a plot

Before the data could be processed, it was filtered to only include the steps that were relevant to the research. Only the steps between 600 and 390 were valid for the 3m test, and the steps between 600 and 250 were valid for the 5m walkway.

Hypothesis 1 and Hypothesis 2

After this was done for each participant and for each patient, the steps were averaged, and these were input into the two-way ANOVA analysis. The formula for the ANOVA analysis was as follows:

$$Average\ steplength = run * length\ of\ the\ walkway$$

The resulting values that were found can be found in Table 8 in *Appendix 16.4 Results*.
These results indicate a significant main effect of walkway length on the average step length (p = 0.003). However, this initial result does not specify which walkways significantly differ from the 7.3m baseline. To further analyze this, post-hoc paired t-tests with a Bonferroni correction were conducted. This analysis showed a significant difference between the 3m and 7.3m walkways (p = 0.005), but no significant difference between the 5m and 7.3m walkways (p = 0.071).
To quantify this impact, Cohen's d effect sizes were calculated. The comparison between the 3m and 7.3m walkways yielded a d = 0.85, indicating a large effect, with the average step length being reduced by 3.86

cm compared to the baseline. The 5m walkway demonstrated a moderate effect (d = 0.56) on the average step length, with a reduction of 2.17 cm.
The number of runs itself had no significant main effect on the step length (p = 0.450).
Furthermore, the interaction effect was not significant (p = 0.077), demonstrating that the patients' step length was not influenced by an interaction between the number of runs and the length of the walkway.

Hypothesis 3
The next analysis aimed to determine if the width of the mat influenced participants' proximity to their step goals, which was the centre of the red cloth. An analysis was done to see if the length of the walkway and the width of the cloth had an influence on the proximity of the foot to the centre of the red cloth.
For the data, the results were filtered to only include the steps of each run for each patient that was closest to the target. After this, the centre of the foot was calculated by subtracting the location of heel contact from the contact point of the toe.
With these findings, a repeated measures ANOVA was done for each axis. The formulas were as follows

$$distance\ X\ of\ target = length\ of\ walkway * size\ of\ the\ cloth$$

$$distance\ Y\ of\ target = length\ of\ walkway * size\ of\ the\ cloth$$

These gave the following results that can be seen in Table 9 and Table 10 in *Appendix 16.4 Results*.
From this, the conclusion can be drawn that neither the width of the scan platform nor the length of the walkway has a significant influence on the patient's ability to place their foot in proximity to the centre of the target since both had a p>0.05. And the experiment results are visualised in Figure 14

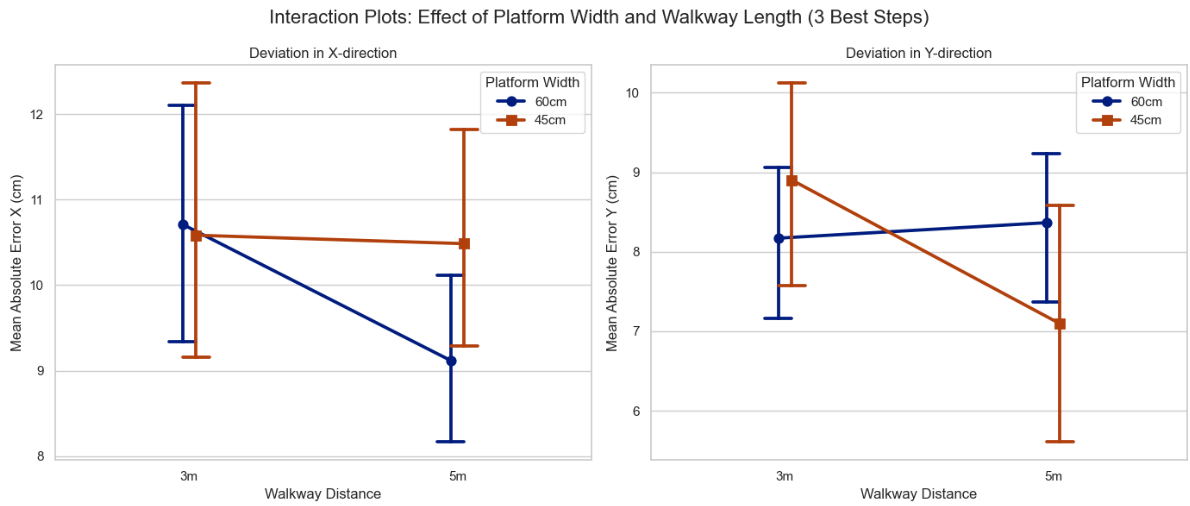

Figure 14 - Interaction Plots: Effect of Platform Width and Walkway Length (3 Best Steps)

Additional Observations
Also, an interesting observation was that all participants would look down while walking due to the assignment given. This could lead to a less natural gait, which in turn could influence results.

7.1.3 Conclusions
From these results, the first hypothesis can be accepted as true, which means the current design of the walkway needs to be lengthened to 5m to ensure that people can walk with a more natural walking gait

The second hypothesis is disproven; this means practice runs are allowed since these don't influence the results. This will enable patients to become more familiar with walking on the scanner, reducing discomfort and might allow for a more natural gait.
The third hypothesis was disproven in the horizontal as well as the vertical direction. However, the size of the deviation shown in Figure 14 shows that the ability of the patient to step into the centre of the platform varies greatly between patients. The distance also implies a bigger scanner is needed to ensure the foot is always within the bounding area. In 6.1.3, the final area was calculated to be 345 x 255mm; this new research shows it needs to be increased to 445 x 255mm.

7.2 The influence of the combined effects of height and width on perceived discomfort

From personal use, a sense of discomfort due to the height and width was felt. To verify the extent of this effect, a study was done with the following hypothesis.

1. The height influences the perceived discomfort of a person
2. The width influences the perceived discomfort of a person.
3. There is an interacting effect between these two variables.

7.2.1 Method


Figure 15 - Participant is standing next to the walkway in vr and tries to visualise the hight

To quantify the subconscious psychological impact of the scanner's physical elevation and width, a comparative Virtual Reality (VR) simulation study was designed. The full methodological details and execution of this study can be read *in Appendix: The influence of the combined effects of height and width on perceived discomfort.*
The experiment was done with 8 participants (3 females and 5 males) within the age range of 20 and 30, with varying heights between 1.6m and 2.1.

Participants were first surveyed for their age, height, self-reported fear of heights, and prior VR experience. Following this, the participants were instructed to put on the VR headset and were instructed to familiarise themselves with the VR set-up and VR environment. Instruction on how to teleport and interact were given; they were given some time to do this, with the hope to immerse themself into the VR world.
After this, the experiment began. Participants had to evaluate a series of platforms, all of which varied in height and width, rating their levels of distress when standing on the platform on a scale from 0 (no distress) to 7 (extreme distress).

7.2.2 Results

A Repeated Measures ANOVA was done to analyse the effects of Height, Width, and their interaction (Height × Width) on the dependent variable. The results can be seen in Table 11 in *Appendix 17.4 Results*. It revealed significant effects of both platform height ($p < 0.001$) and width ($p < 0.001$) on perceived distress, with width having a more pronounced influence.

A significant interaction effect ($p < 0.001$) indicated that height and width influenced discomfort in an interdependent manner. This effect can be seen in Figure 16.

It was also observed that the participants would instantly rate the floor as a zero, as they required time to rate any platform above that. This indicates that they might unconsciously experience a slight discomfort but couldn't adequately rate it, which led to them doubting between 0 and 1 and hence the slight delay in scoring anything above the floor. However, the previously explained point is only conjecture.

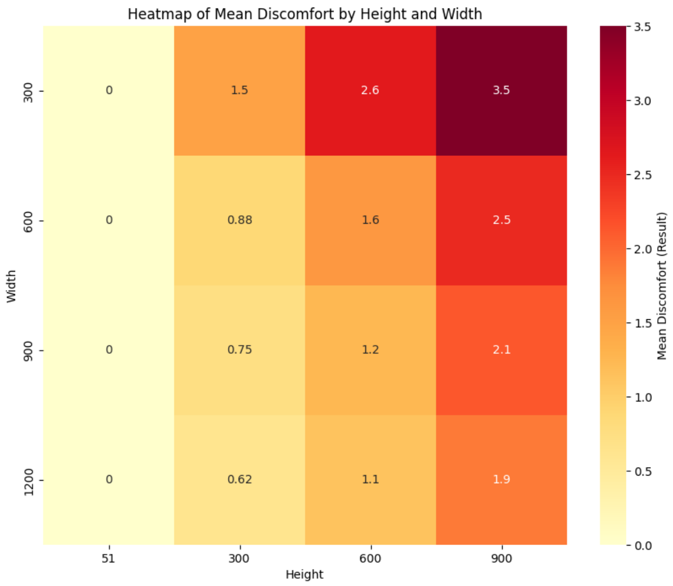

Figure 16 - Heatmap of mean discomfort by height and width

7.2.3 Conclusions

From this experiment, the conclusion can be drawn that all hypotheses are confirmed.
This means for the design that a walkway that is level with the ground is preferred, or alternatively a platform that is as low and wide as possible.

7.3 Resulting Design Requirements from second foot placement study and VR-study

Based on the dimensional influences on the patient's gait and perceived discomfort, the following points provide concrete design requirements:

- **Walkway Length:** The walkway must be lengthened to at least 5 meters to ensure patients can perform a natural gait cycle, as shorter lengths significantly reduce their final step length.
- **Scanning Area Dimensions:** Because the ability to step exactly in the center varies greatly between patients, the transparent scanning area must be enlarged to at least 445 x 255 mm to guarantee the foot is always captured within the bounding box.
- **Platform Height and Width:** To minimize subconscious distress and fear of falling, the platform should ideally be flush with the floor. If elevation is mechanically necessary, the platform must be designed to be as low and wide as physically possible.
- **Familiarization (Clinical Procedure):** The design and clinical procedure should accommodate practice runs, as repeated use of the walkway does not negatively alter the patient's step length and helps reduce discomfort.

8 Requirements and wishes definition

In this chapter, the findings from the preliminary research are translated into a concrete set of requirements. The theoretical insights and practical constraints discussed in the previous chapters will form a guideline for the physical and technical development of the new 4D foot scanner. To show exactly where these parameters come from, each requirement listed below includes a direct reference to its corresponding section in the research.

8.1 Requirements

8.1.1 Mechanical requirements

The walkway will be subject to forces due to the patients walking. The walkway needs to be able to resist these forces in the required directions

- The frame must be able to resist peak forces of 5200N in the Z direction and forces of 800N in XY plane. (4.6).

8.1.2 Scanner Mounting

To ensure the accuracy of the final 3D models, the physical mounting of the cameras must be stable. As found in the previously done research, vibrations produced by the patient walking reduce the quality of the depth data. Also, the framework must allow precise alignment of the cameras to generate a good point cloud.

- The mounting solution needs to prevent the vibrations of the walking platform from reaching the cameras(3.4).
- The mounting solution needs to help align the cameras accurately within 1 degree.

8.1.3 Scanner Positioning

In 6.2, the optimal camera positions were calculated for the walkway. These positions need to be the basis for the placement of the cameras.

- The camera's position must be according to the locations provided in 6.3.

8.1.4 Scan area size

Currently, the scanner area is undefined. However, the experiment showed that people step into an area of 444 mm by 225 when instructed to aim for the centre of the plate, as demonstrated in 7.1.2.

- The scanner set-up needs to be aimed at an area of 445mm by 225mm (7.3).

8.1.5 Walkway Design, Safety, and Accessibility

The new design of the walkway must focus on patient safety, hygiene, and the collection of natural gait data. The dimensions are determined by the space needed to capture a full stride, while the placement and surface materials are determined by the clinical environment and the needs of mobility-impaired patients.

- The scanning area must consist of a transparent platform (e.g., glass or acrylic) to allow the bottom-up scanning method, keeping the design that was validated by Kwa (2021)

- The walkway needs to have a minimal length of 5 meters to ensure the participant can perform a natural gait (7.3).
- The surface of the walkway must not react to cleaning agents (5.1.1).
- The walkway must be safe for the participant to walk over and accessible to people with impaired mobility (5.1.1).
- The walkway surface needs to be free of interruptions (5.1.1).
- Ensure the component count is as low as possible for fast deployment (5.1.1).

8.1.6 Camera specifications

The quality of the dynamic foot morphology scan depends on the hardware. The current specifications of the Intel RealSense D435i are not enough. To prevent important data from being missed due to the low framerate, the new framerate needs to be at least 30 fps. The focal length of the current scanner greatly influences the final height of the walkway. Preferably, this is as short as possible to ensure the height of the walkway stays as low as possible.

- The system needs to be able to capture the gait at 30 fps (3.4).
- The system needs a higher resolution than the Intel RealSense D435i (3.4).
- The bottom scanner needs to have a focal length less than 28cm (3.4).

8.1.7 Transport

Due to the fact that the scanner needs to be able to be transported. This means it needs to be able to be dismantled.

- To make sure it fits in a car (example Volkswagen Polo), the longest part of the walkway may not exceed 1 meter. (5.1.1).

8.1.8 Cost and Economic Viability

One of the core objectives of this project as a whole was to design a low-cost scanner for podiatric use. To ensure the final design is financially viable and competitive with other alternatives, the final cost needs to be as low as possible

- The total manufacturing and component cost (Bill of Materials) of the physical scanner setup (including cameras, extrusions, walkway materials and the processing PC) must not be more than €30.000 (2.3).

8.1.9 Clinic Integration and Walkway Height

As the research has shown in 7.2.3, the design needs to be flush with the ground to eliminate any influence on the gate. However, big modifications like making recesses in the clinic's floor are impractical and often expensive. This makes the design less viable for practical use. To eliminate this issue, the new design needs to be as low to the floor as possible without any significant alterations for the clinic. This also ensures patients with limited mobility can easily access the walkway.

- The walkway system must be designed for placement directly on top of an existing floor, requiring minimal modifications to the clinic (7.2.3).
- The physical step-up height of the platform must be minimised as much as possible to maximise accessibility and patient comfort (5.2.1).

9 Scanner choice

The purpose of this chapter is to explore the different scanners. As noted in Chapter 3, the current quality is not sufficient for the scanner to achieve sub-millimetre resolution. A potential avenue to explore is the choice to switch from the currently used Intel RealSense D435 to another scanner. There are several aspects that are important for the choice of a new scanner.

9.1 Scanner comparison

To overcome the resolution and framerate bottlenecks of the previous prototype, a hardware upgrade is essential. This section compares several modern depth sensors against the baseline Intel RealSense D435i. The overarching objective is to identify a commercial scanner that can consistently capture dynamic morphology at a minimum of 30 frames per second, whilst remaining within the strict financial budget of the clinical target audience.
The project already had the Azure Kinect as a preference; however, in time, this scanner was superseded by the Femto Bolt with a more advanced model called the Femto Bolt Mega. This model is not compared due to its high price compared to all the other scanners. The resulting table can be seen in *Table 12 - Scanner comparison in Appendix: Scanner general comparison*.

9.2 Calculation of the highest resolution scan

Merely looking at a camera's advertised resolution is not sufficient to guarantee high-quality 3D scans. To ensure the selected camera can actually capture the sub-millimeter details required for orthotic insoles, the effective pixel size directly on the scanned surface must be quantified. This true scanning density is dependent on several aspects of the scanner: the resolution, the field of view (FOV), and the minimum focal distance. By calculating the estimated area of the pixels on the scanned subject, a scientifically grounded hardware choice can be made.
First, the length of one side of the plane is calculated at a distance for each angle of the FOV

$$Length\ of one\ side = 2 * distance * tan(Angle/2)$$

Afterwards, the resolution can be used to calculate the height and width of each pixel

$$Onse\ side\ of\ the\ pixel =\ Length\ of one\ side/resolution$$

It is an estimate, since if the subject is farther or closer than the plane used to calculate the resolution, the pixel size will change.

In Table 12 - Scanner comparison in *Appendix: Scanner general comparison*, several scanners are compared with each of their modes. The Azure Kinect is already eliminated as a choice since it is no longer available and, as such, won't be in the comparison. The distance used will be the furthest distance that is currently calculated by the Farzam algorithm from the centre of the scanner plate to the emitter of the scanner. Currently, that distance is 75cm. As well as the average distance, which is 50cm. The full calculations for each mode, for each device at the previously mentioned distance, can be found in the *Appendix: Pixel size calculations for the scanner comparison*.

The results show the ideal mode for each device at each distance. It shows that even though a higher-resolution depth scan is possible, it does not provide the highest resolution of the surface of the object itself. The settings with the highest and second highest resolution at the earlier mentioned distance are put in Table 2.

Table 2 - Highest Scoring options scanners and their relevant modes

	Resolution	FOV	Pixel Size (mm) 750 distance	Area (mm^2) at 750 distance	Pixel Size (mm) 500 mm distance	Area (mm^2) at 500 distance
D435 High res	1280 x 720	87 x 58	1,11 x 1,15	1,28	0,74 x 0,77	0, 57
D435 High Speed	848 x 480	87 x 58	1,68 x 1, 73	2,91	1,12 x 1,15	1,29
Femto NFOV unbinned	640 x 576	65 x 75	1,49 x 2,00	2,98	1,00 x 1,33	1,33
Femto WFOV unbinned	1024 x 1024	120 x 120	2,54 x 2,54	6,44	1,69 x 1,69	2,86

As can be observed from Table 2, the D435 appears to be the superior choice in matters of resolution and the speed at which it can capture data. However, the choice needs to be made with several factors in mind. To facilitate this decision, a Harris profile was done. This can be seen in Table 3 - Harris Profile concerning scanner choice.

Table 3 - Harris Profile concerning scanner choice

	D435 (High Res)					D435 (High Speed)				
Edge quality	■	■				■	■			
Area of pixel			■	■				■		
Fps			■					■	■	
Sync method	■	■				■	■			
Sync cable	■	■				■	■			
cost			■	■				■	■	
	Femto Bolt NFOV					Femto Bolt WFOV				
Edge quality			■	■				■	■	
Area of pixel			■			■	■			
Fps			■					■		
Sync method			■	■				■	■	
Sync cable			■					■		
cost	■	■				■	■			

The Harris profile shows that the best solution is the Femto Bolt in NFOV mode.

9.3 Final design conclusion

The femto bolt in NFOV seems to be the best option. However, some concepts were formed with the idea of implementing mirrors in the following chapter. It will be explored in this use case that the Femto bolt is the best option.

10 Advanced concepts validation

To maximize the cameras' field of view and minimize the physical step-up height of the walkway, unconventional optical setups, such as the integration of mirrors (catadioptric systems), were hypothesized. This chapter evaluates these advanced theoretical concepts against known optical principles to determine whether they offer a practical, viable solution for the redesigned scanner without compromising 3D data fidelity

10.1 Concept explanation

The current scanner set-up utilises only the centre portion of the scanner's field of view for data capture. However, most depth scanners have additional wide-view modes that allow for more data to be captured. This, however, comes at the cost that the accuracy drops the closer you get to the edge of the frame. This is caused by the distortions caused by its lens (Thabet et al., 2014).

Far-away reflection

One concept design could be to utilise this “left-over” peripheral view and use it to capture additional data of the foot. This can be done by the use of mirrors (also called a catadioptric set-up) that could reflect the depth scanning pulses to the foot. By doing this, you can create additional “virtual” cameras that would allow for additional viewpoints of the foot to eliminate blind spots during the scan (Kontogianni et al., 2018). Potential downsides are that a “ghost” of the foot will be captured at the perceived distance behind the mirror plane. These effects need to be compensated for and can be done by complex spatial transformations to align the “ghost” foot with the real foot.

Close-by reflection

Another concept could be the opposite of the one just mentioned. Instead of putting the mirrors far away from the scanner, place the mirrors close to the scanner.
By reflecting the pulses immediately, the beams will diverge less, which would in theory, help to maintain accuracy while creating the additional virtual cameras.
The potential downside is that you could create a light trap. This would cause the pulses to be bounced around multiple times before returning to the sensor. This is called Multipath interference (MPI), and its effect can be described as if the data were from a kaleidoscope.

Mirror for the bottom Scanner

This concept is an extension of the previous concept. Currently, the focal length of the scanner defines the height of the walkway. If it is not possible to find a scanner with a reduced focal length that matches the needed requirements, an option would be to use a mirror to extend the focal length of the scanner while simultaneously reducing the height of the walkway.

All of these concepts are dependent on the use of mirrors. This could be beneficial and potentially increase the density of the scans done and, as such, the fidelity of the scans.
However, all these benefits are theoretical, and that is why, in this chapter, a study was done to see if these concepts are feasible.

10.2 Issues of mirrors

Several new issues are introduced due to the use of mirrors, which need to be accounted for.

Dust/debris
Mirrors can collect dust, dirt or fingerprints on their surfaces, which can reduce the accuracy of the scanner's measurements. These containments can cause depth errors or noise in the data, which has knock-on effects on the quality of the scan.
To prevent this from happening, frequent inspections and/or cleaning are needed.

False reflections
The structured light can reflect off the object onto the mirror and back again. This can cause “false points” of data in the scan. These secondary reflections can be as bright or brighter than the original scan rays. So this makes them hard to recognise by just checking on the brightness of the ray alone.
As was demonstrated in Wallace et all, false reflections due to this issue can show incorrect locations. This leads to outliers in the depth data for the 3d scan. These mirror reflections can cause phantom surfaces or distortions and need to be identified and filtered out by software to ensure the quality of the scan.

Calibration and software compensation:
Because a mirror changes the distance measured by the depth scanner, a spatial transformation needs to be applied to the data it acquired to ensure it is usable. To perform this transformation correctly, the mounting of the mirror needs to be precise and repeatable between dis- and assemblies. Also, the mirrors' planes' location and orientation must be known beforehand. This spatial information is needed so the point cloud can be transformed to the shared coordinate system.
Thomaidis (2014) developed a “Mirror Transformation” algorithm to automate this step (G. Kontogianni, 2018).
If this design is implemented, then these systems need to be able to accurately place and tilt the mirrors to ensure the highest quality scans.

Mirror quality and type:
To further increase the accuracy of the scan, a first-surface (front surface) mirror must be used. Household (back-surface) mirrors have a layer of glass over the reflective layer. This causes the incoming pulse to be refracted twice. Once when entering and once when leaving the glass layer. This causes the pulse to be shifted over, thus creating erroneous measurements. (G. Kontogianni, 2018).
The first-surface mirror has, as its name implies, the reflective layer on the front. This eliminates the refractive issues. This ensures that the reflected image is “true” to the original object.
Its downside is that due to the elimination of the protective glass layer, these mirrors are more susceptible to scratches and damage, and as such must be handled carefully. (G. Kontogianni, 2018).

Added cost:
Front surfaces are more expensive than their back-surface mirror counterparts. Since this project aims to design a low-cost 4D scanner, this is less desirable. Depending on the concept chosen, the added cost would be small (close-by mirror/bottom mirror) or quite significant (Far-away mirror) due to the difference in the size of the needed mirrors.

10.3 Femto Bolt specific issues

The previously selected Femto Bolt uses Amplitude Modulated Continuous Wave (AMCW) Time-of-Flight (ToF) to generate depth maps. While this sensor technology offers high resolution and ensures that depth measurements stay consistent and don’t flicker over time, it suffers from issues in catadioptric (mirror-based) set-ups. Several of these issues are explained in the paragraphs below.

Multipath Interference (MPI)
As alluded to before in the introduction from Concept 2, MPI might be challenging for the Femto Bolt. The depth calculating algorithm assumes that every emitted photon, for each pixel, travelled in a straight line from the emitter to the object and back (Hansard, 2012).
In a mirror setup, and especially with the Concept 2 light trap, this assumption won't hold. The signal will bounce multiple times between the mirrors and the object before returning to the sensor. Because the sensor will average all the returning phase shifts of each photon (phasors) over a certain exposure time, the result will be a calculated distance that doesn't match reality (Xu, 2018).
This shows itself as straight surfaces becoming curved and edges becoming more rounded. This is detrimental to the final fidelity of the scan. Xu (2018) recommended for these set-ups the use of pulsed ToF (pToF). This differs by the fact that the Femto Bolt averages the phase shifts from a continuous stream of light. pToF only takes the value of the first returning pulse. Since the direct path is always the shortest, the first returning pulse will represent the true distance from the object. This will effectively filter out any unwanted delayed reflections (Xu, 2018).

Mixed Pixels and "Flying Pixels"
Another common issue enhanced by mirrors is the "flying pixel". This occurs when the depth measurement is done at an edge of an object, in this case, the boundary of the foot or a mirror. When a single pixel lands partially on the frame of the mirror and the wall behind it, the sensor will receive two depth values simultaneously. Instead of taking one value, the scanner will again average these phase shift values. This will result in an invalid value that manifests itself as a point that floats in "mid-air" between the two surfaces it tried to measure (Tölgyessy, 2021). In catadioptric systems, these flying pixels can create a halo of noisy data around the contours of an object (Sarbolandi, 2015).
This phenomenon can also occur when aiming the scanner through a glass plate. This happens with the bottom scanner that is needed to scan the bottom of the foot.
Removing this noise from the data can be done with strong filtering algorithms, but these might erode the contour of the foot. This will reduce the needed accuracy for the high-fidelity scans that are needed to create an orthopaedic insole.

Both of these issues make the Femto Bolt ill-suited to be used in combination with this concept.

10.4 Alternative Sensor Technology: Active Stereo Vision (Intel RealSense)

While the Femto Bolt (ToF) is ill-suited for these concepts, an alternative needs to be found that can be implemented for use as the bottom scanner. The previously discussed Intel RealSense, which uses ASV, might be suitable. Unlike the Femto Bolt, which measures phase shift variance, ASV does its depth calculation through triangulation of the captured images and the scanner's lenses (Kumar, 2024). The results of the Intel RealSense are further enhanced by the fact it uses an infrared pattern to texture objects. The Intel RealSense is not susceptible to the issues such as the aforementioned MPI of the Femto Bolt.

10.4.1 Immunity to Multipath Interference in Mirror Setups

The core advantage of ASV in mirror-based scanning (Concept 1 & 2) is its resistance to signal corruption from reflections.

Geometric Consistency
As mentioned before, Stereo Vision systems calculate the depth and the shape of the final object with the use of the images captured, combined with an algorithm that checks for matching features.
A mirror image is just light rays bouncing from the mirror plane. The system will create a "virtual object" behind the mirror plane that follows the shape of the object.

Because the algorithm depends on the use of these visual features, and the mirror images display these, it can calculate the depth and shape of the object. This is how this system is immune to issues caused by mirrors.

No "Light Trap" Effect

In the proposed pyramidal setup (Concept 2), as mentioned before, a continuous-wave ToF sensor would fail due to the emitted light bouncing multiple times before returning, which disrupts the phase-shift calculations.

An Active Stereo Vision (ASV) sensor, however, is passive in its depth calculation. It does not rely on the precise timing of light waves. As long as the foot's textured reflection is visible in the mirror, the depth can be calculated. Because scattered multiple reflections do not form matching features across the camera views, they are ignored by the stereo matching algorithm.

10.4.2 Transparent mediums (Glass/Polycarbonate)

For scanning the foot sole, the sensor has to look through and see through a medium, which could be glass or another material.

When a ToF sensor transmits light through a transparent medium, a portion of the signal reflects off the glass surface, while the rest travels to the foot and back. The sensor receives both signals and averages them, resulting in a depth measurement that lies erroneously inside the glass plate or "ghost" noise (Hansard, 2012).

ASV systems are inherently better at "seeing through" transparent media. The cameras focus on the texture of the skin (the foot sole), which has high contrast due to the projected IR pattern. Since a transparent medium lacks texture, the stereo matching will focus on the foot surface instead, which is behind the glass.

10.4.3 Hardware Recommendations for Foot Scanning

Based on the constraints for the height of the platform that were found in 7.2.3 which showed that a scanner with a minimum focal distance was needed to ensure the platform stays as low to the ground. The Intel RealSense D405 was found to be a good fit on paper for this task due to its short focal distance of only 7cm at which it promises sub-millimetre accuracy (Corporation, 2022).

And in this regard, it is superior to the Femto Bolt and Intel RealSense D435, which need a minimum distance of 25 cm and 28 cm, respectively.

However, the surfaces it scans also need to adequately cover the scan plate so the whole foot can be captured.

To calculate the distance needed to capture an area with the longest side of 45cm with the D405, the formula is as follows:

$$\mathrm{d} = \frac{L}{2 \times \tan\left(\frac{a}{2}\right)}$$

In this formula, the d stands for the focal length, the L for the value of one side and a for the angle filled in. The D405 has an FOV of 87 by 58 degrees. If all parameters are filled in, the result shows a distance of 23,7 cm (at an angle of 87 degrees). By rewriting the formula, the length of the other side can be calculated

$$L = d * 2 * tan\left(\frac{a}{2}\right)$$

If these numbers are filled in (d=23,7 and a=58 degrees) the final result is 26,3. At this size, the requirement mentioned in 7.1.3 would be satisfied.
However, at this distance, the only benefit that is gained is the ability to scan through the glass, and it is not a superior option compared to the other previously explored scanners.

A solution to this issue is to halve the distance and use 2 scanners to come to a comparable scan area. The added cost is high, but the benefit is that due to the shorter scanning distance that can be implemented, the height of the walkway can be lowered, and the accuracy of the scan will increase. An additional benefit is a decrease in cost and environmental impact, since less material is needed for the legs.
Since the most important area to capture is the sole, the choice is made to continue with 2 scanners on the bottom with a distance to the foot of 11,85cm.

10.5 Conclusion

For the proposed catadioptric designs, Active Stereo Vision(D405) is the technically superior choice. It eliminates the fatal Multipath Interference issues inherent to ToF (Femto Bolt) and allows for a compact mechanical design due to lower minimum-distance requirements.

10.6 Final design conclusion

Since, from personal communications, it was made clear that the Femto Bolt has the preference, the choice was made to eliminate these concepts since they would not be feasible. However, the choice was made to replace the bottom camera with 2 Intel RealSense D405. Since it short range applications allows for the walkway height to be reduced significantly, as well as its resistance to issues with the glass plate. This does make the software integration more complicated; however, those issues will be ignored, since they are outside the scope of the project.

11 Walkway design exploration

Currently, the focus of the design is on the scanners. However, the walkway needs to be redesigned based on the findings from the previously done research. Also, as mentioned in the introduction, the support for the scanners needs to be redesigned as well to reduce the vibration of the cadence of the patients to influence the fidelity of the scan. Since this is a large interconnected aspect of the design, the choice was made to split it into chunks and iterate on the parts as needed. The segments are as follows: The walkway, supports for the walkway, scanner mounting and smaller adjustments to the design that do not fit into these larger segments.

11.1 Modular walkway design

To fulfil the critical requirement of field portability, the redesign must feature a modular architecture that allows the entire setup to be dismantled and transported in a compact vehicle. However, segmenting the walkway introduces significant structural challenges. This section details the design exploration of the modular platforms, ensuring that the new segmented frame remains rigid enough to safely resist the previously established dynamic peak forces (5200 N vertically and 800 N laterally)

11.1.1 Surface of the walkway

In the design from Kwa(2021) the surface is made from 15mm hardwood this aspect is taken over from the old design. An addition is made to the new design, is by making the top layer from vinyl sheeting. This is done so it is compliant with the requirement mentioned in 8.1.5.
This ensures the surface doesn’t get damaged due to the cleaning agents needed to ensure hygienic operations, as well as reduces the amount of surface pores in which harmful bacteria can settle.
On the vinyl is also made a line that will help ensure the patients walk in a straight line while doing a scan. This line isn’t all the way over the walkway, only on the 2 end platforms, so people have a goal to walk towards.

11.1.2 Dimensions and segmentation of the walkway platforms

To ensure the disassembled frame fits within the trunk of a compact car (e.g., a Volkswagen Polo with the couches down*)*, the walkway is constructed of a modular assembly. This allows for easy dismantling for transportation.
The new total length of the walkway is 5m to ensure the natural gait of the patient can be captured while accounting for the acceleration and deceleration of the gait. The walkway is segmented into several parts:

11.1.3 Iterative approach

To start the design, a dimension of the walkway was chosen to provide some baseline that can be changed during the process and can be used to test and validate design ideas against.

Initial design

Central walkway platform: 1000mm x 600mm. These dimensions minimise the number of joints the patient must step over, reducing psychological barriers that could influence gait patterns (as observed in Chapter 10). The final dimensions are chosen by trying to maximise the size that could fit in the Volkswagen Polo, and simultaneously minimising the number of parts needed for the central walkway.

Scanner platform: This design is kept the same as Kwa's (2021) design because it is sufficient for its purpose and has also been validated.

Widening Segments: Additional side panels increase the effective width to enhance patient stability and comfort, addressing the "fear of falling" constraint identified in the VR study. These come in 2 sizes. One is the 200 by 1000mm to widen the central module, the other is 200 by 600mm to widen the scanner module.

Final dimensions

Initially, the central walkway platforms were designed at 1000x600 mm, flanked by narrow 200 mm widening segments. However, as will be demonstrated in the structural force analysis in Section 11.2, heavy-duty L-extrusions (45x90x90 mm) were required to support the frame against dynamic loads. These robust support legs were physically too large to fit securely underneath the narrow 200 mm widening platforms. Consequently, the final design iteratively shifted to utilizing standardized platforms of 400x1000 mm exclusively. By placing three 400 mm modules side-by-side, the overall required walkway width of 1.2 meters is successfully maintained, while ensuring the large L-extrusions fit perfectly under every load-bearing corner.
Due to this change the scanner platform dimensions and the pieces flanking it are changes as well in size to 600mm by 400mm.

11.1.4 Extrusion size

Due to the goal of the project to keep the cost as low as possible, the decision was made to compare the currently used 5050 to 4545. From personal communications and Vidmar (2020), concerns were raised regarding whether thinner extrusions would vibrate due to the cadence of the patients. To mitigate any concern about vibrations that could be transmitted through the frame, the option was to only compare the closest extrusion in size.

Table 4 - Cost comparison of the frames between extrusion sizes

Extrusion type	4545	5050
Big Platform V1	197,28	315,6
Small Platform V1	307,20	479,71
Smallest Platform	54,96	77,848
Scan Platform	38,40	57,86
Total	**597,84**	**931,02**

Table 4 shows the total cost for all the different types of platforms. The costs here are calculated for the initial platform design, not for the final platform design, as mentioned in 11.1.3. The cost calculated here is only the extrusions and a potential connector to form the frame. The total table with all the parts can be found at *appendix chapter 24.*
As can be seen, the 5050 extrusion platforms are 1,5 times as expensive as the 4545 extrusion, and this is withholding the connectors since a price could not be found for these at the 5050 size. Due to the potential cost savings, the choice was made to go forward with the 4545 extrusions for the final concept design.

11.1.5 Frame connector

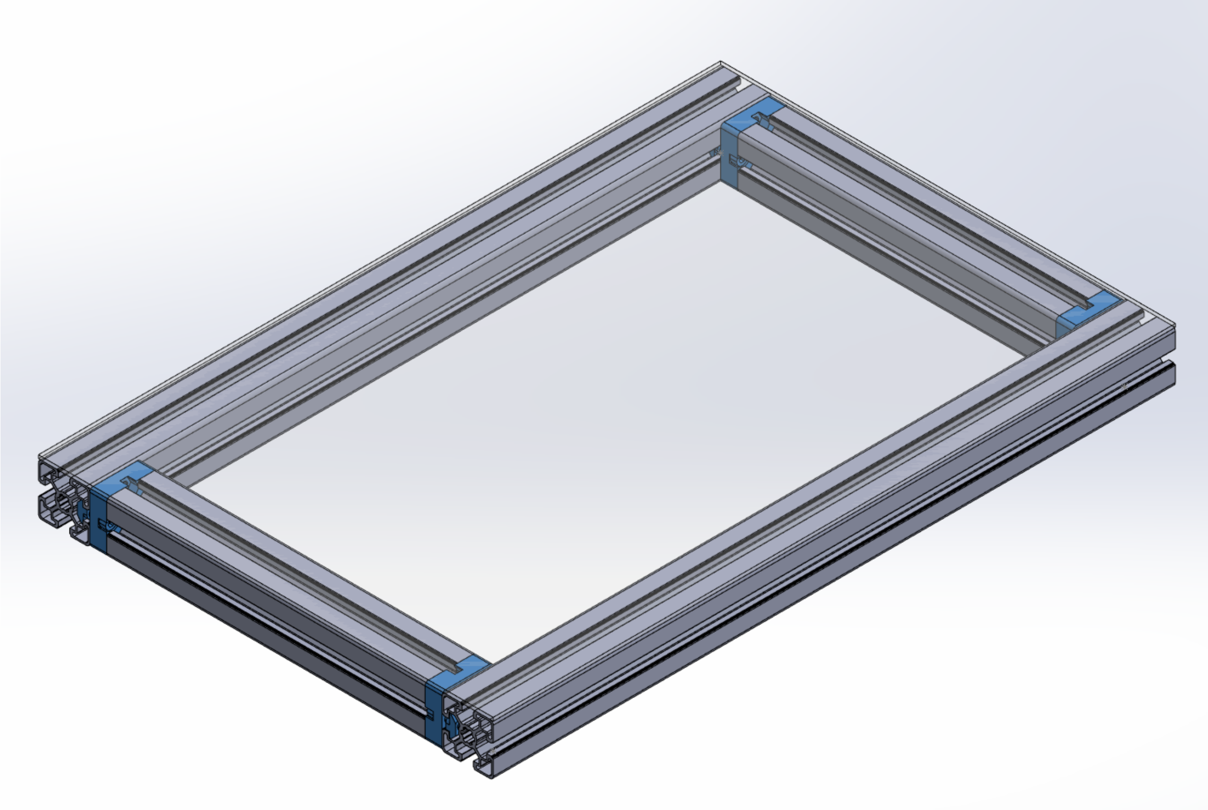

Figure 17 - Illustration of the frame used for the scanning platform and a potential connector indicated with blue (t-joint)

To connect all the extrusions of the modular pieces of the walkway, an analysis was done to find the most suitable solution for a connector. A situation example can be seen in Figure 17. The purpose of the connector is to withstand the forces defined in Chapter 8.1.1. A force analysis is done to see which solution is most suitable.

Worst-case scenario loading and mechanical principles

When the 800 N horizontal braking force is applied to the continuous long side (L= 1m), it behaves as a simply supported beam. This is because the corner connectors are mounted into the side-slots of the continuous profile, which cannot act as perfectly rigid fixed supports against bending. Therefore, the theoretical maximum bending moment is calculated using the baseline formula:

$$M_{max} = \frac{F * L}{4}$$

This yields a maximum horizontal bending moment of 200 Nm at the center of the beam, which is safely absorbed internally by the structural stiffness of the aluminium profile itself. The connectors at the ends primarily only need to resist the horizontal shear force (400 N per connector) and provide sufficient corner rigidity to prevent the frame from skewing into a parallelogram. To evaluate which off-the-shelf connector provides the safest corner connection under these lateral loads, a structural capacity analysis was performed (Appendix 19). The T-joint was selected as the optimal solution because its structural moment resistance (~200 Nm) provides a massive safety margin for corner rigidity, while remaining highly cost-effective and easy to assemble.

11.1.6 Height

As established in 10.5, the choice was made to implement 2 D405 for the bottom scanner. This choice was made to reduce the overall height of the walkway compared to when a Femto bolt would be implemented.

To implement this solution, the scanner distance to the top of the glass plate has to be at least 140mm. Accounting for the housing of the D405, the surface of the glass plate needs to be 163 mm from the ground

But this choice also provides additional benefits that weren't discussed in 10.5. Due to the shortening of the focal distance, the height of the walkway can be lowered, which allows for easier access to the walkway for patients with mobility issues. This would also reduce the amount of discomfort patients would experience due to being on the platform, as established in 7.2.
The reduction of the height also creates a quite significant cost saving due to the reduction of needed materials. The current iteration has 15 platforms; each walkway has 4 legs, totalling 60 legs that are needed. So a small reduction in material has a big influence on the total amount of material needed and thus its cost. And due to the reduction of the materials needed, a significant reduction in its environmental impact is achieved as well.

11.2 Supports for the walkway

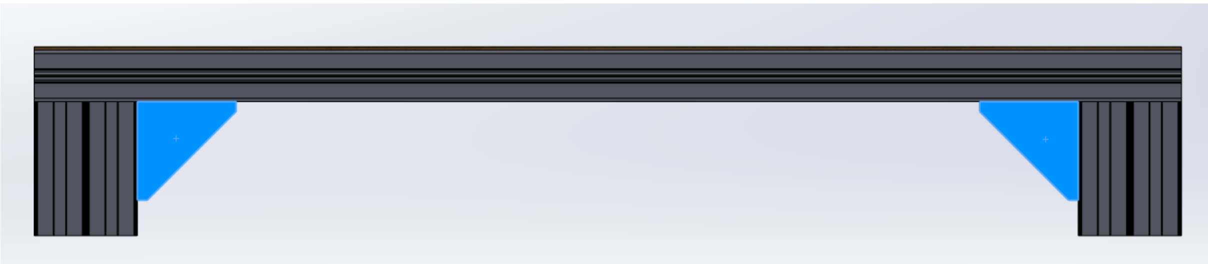

Figure 18 - Illustration of the legs and frame, and a potential connector to connect them, indicated with blue (bracket)

11.2.1 Feasibility forces analysis

Lateral Load and Movement

As established in 4.4 and 4.6, the walkway will experience forces in the lateral plane due to the force applied in the heel strike phase of the gait. The requirement for the walkway to be able to resist was set to 800N in the lateral plane. This is the value that will be used for the following analysis.
Because the walkway is a freestanding structure, in practice, the walkway would shift in the lateral plane before any joints reach any critical stress levels. However, this might introduce a new issue; due to the shifting of the walkway relative to one another, issues could arise with the calibration of the camera system. This is why any solution needs to be rigid enough to prevent this issue from occurring.
The vertical load was set at 5200 N in 4.4 to account for the forces created by the patients' walking. Due to the size of the force, it will create a significant moment which the connector needs to be able to compensate for.

Vertical Load and Leg-to-Frame Support Mechanics
To provide stable elevation for the walkway, vertical support legs must be connected to the modular frame. Initially, a standard assembly method (Concept A) is evaluated, where four individual legs are attached to the corners of the platform using off-the-shelf brackets. To validate if these leg-to-frame connectors can safely carry the walkway, the maximum dynamic vertical point load of 5200 N (*Fdownward*) is applied to the platform.

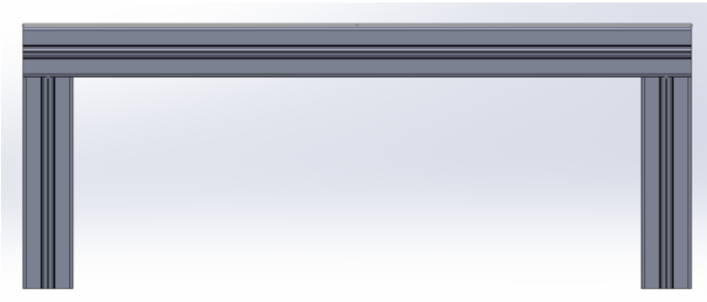

Figure 20 - Situation of the long side of the frame

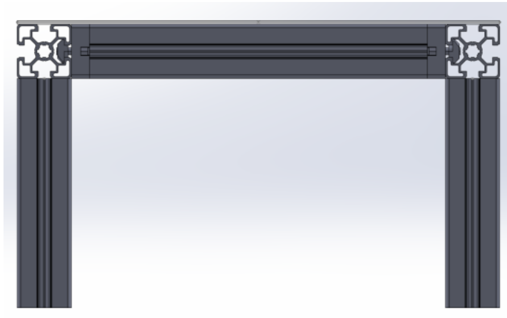

Figure 19 - Situation of the short side of the frame (the middle beam is unsupported by the legs)

Because the frame is rigidly clamped to these legs, the vertical downward force creates two critical stresses on the leg-to-frame connectors: vertical shear force and bending moment.
Assuming the 5200 N load is applied in the center of the platform sides, static equilibrium distributes this load equally across the supports. This results in a maximum vertical shear force (Vmax) of 2600 N that the connectors on each side must physically carry.

Furthermore, as the platform bends under the 5200 N vertical load, the entire structure acts as a rigid fixed frame because the horizontal beams are rigidly clamped to the vertical legs using corner brackets. The theoretical maximum vertical bending moment is therefore calculated using the formula for a fixed-ended beam:

$$M_{max} = \frac{F * L}{8}$$

This bending enforces a massive rotational moment directly onto the leg-to-frame brackets in the *xz*-plane. For the continuous long side (L= 1m), this results in a peak vertical bending moment of 650 Nm. For the short side (L=0.51 m), this yields a bending moment of 331.5 Nm.
Therefore, to successfully mount the legs to the side of the frame using standard fasteners, the chosen bracket must be able to resist at least 2600 N of vertical shear force and up to 650 Nm of vertical bending moment.

11.2.2 Design exploration
To make sure the walkway stays modular and stable, several design options were explored. The design concepts were focused on reducing the assembly complexity while maintaining the needed structural integrity for clinical use.
The only purpose of the connectors on the long side is to reduce any moment in the lateral plane so the forces can be handled by the vertical support. The above-mentioned forces need to be handled by the connector itself on the short side of the platform.

Each concept will be a different approach to the given problem.

Concept A: Standard Fasteners

This concept focuses on standard components, which are off-the-shelf solutions to create the modular joints. These solutions assume each platform has 4 individual legs.

- A1 Cube connectors: Cube connector allows for easy initial assembly; however does not allow for the legs connector, so this solution is discarded.
- A2 Brackets: 45x45 45x90 45x180. Brackets are easily accessible and easy to assemble.
- A3 T-connectors: Allow for easy assembly as well due to only needing 2 connecting screws.

Any of the above solutions needs to be paired with any of the following solutions to ensure the walkway does not start to drift from one another. All these solutions connect two extrusions.

- A4 Plate connectors: A plate with two holes that allows two separate extrusions to be connected.
- A5 Parallel bar connectors: A bar that is slotted between two extrusions and set by tightening one bolt.
- A6 Parallel connectors: a bolt that is inserted in an extrusion; to access the bolt for tightening, holes need to be drilled through the extrusion.

Concept B: Variation of extrusion dimensions

Instead of focusing on just connectors and only using the 4545 extrusions, other dimensional extrusions can be used to reduce the parts count and thus complexity for assembly. 9090 extrusions can be used for 4-way junctions, and 4590 extrusions can be used for 2-way junctions. The bigger extrusion size also allows for the use of bigger brackets and thus further increases the stiffness of the frame.

11.2.3 Concept validation

A structural capacity analysis was conducted to determine if the proposed off-the-shelf brackets (Concept A) could safely attach the legs to the frame under the required 2600 N shear force and the peak vertical bending moments (up to 650 Nm on the long side and 331.5 Nm on the short side). As detailed in *Appendix 20 (Comparison overview connectors for the legs to the frame*), none of the standard brackets possessed the required structural stiffness to support these extreme rotational moments. Consequently, Concept A is eliminated due to its inability to guarantee patient safety.

Concept B (varying extrusion dimensions, such as using robust 90x90 extrusions for the vertical legs) is also eliminated in its current form. While a larger corner extrusion increases overall stiffness, its physical layout only allows it to directly support one of the intersecting frame beams (the continuous long side). The short side extrusion would still remain suspended. As a result, the previously selected T-joint from Section 11.1.5 is still forced to hold the entire vertical load and absorb the 331.5 Nm vertical bending moment of the short side. Because the T-joint has a maximum structural capacity of approximately 200 Nm, it would critically fail under this load. This identical fundamental load-path issue occurs with any other varied extrusion sizes as long as the short beam remains unsupported.

11.2.4 New potential concept solutions

To determine if the proposed off-the-shelf connectors (Concept A) could safely attach the legs to the frame, their structural capacity was evaluated against the required 2600 N shear force and the peak vertical bending moments (up to 650 Nm on the long side and 331.5 Nm on the short side). As detailed in *Appendix 20 (Comparison overview connectors for the legs to the frame)*, none of the standard brackets possessed the required structural stiffness to support these extreme rotational moments. Consequently, Concept A was eliminated due to its inability to guarantee patient safety under dynamic loading.

The final and most structurally sound solution is the use of four vertical L-shaped extrusions (45x90x90) acting as robust support pillars. Instead of using vulnerable brackets to hang the frame off the side of the legs, the load path is fundamentally redirected. The modular frame is positioned directly *on top* of these L-

extrusions. Because the vertical forces now travel straight from the aluminium frame directly into the support legs and down to the floor, the leg-to-frame connectors are entirely relieved of the 2600 N shear force and the massive bending moments.
However, these robust L-extrusions could not be safely integrated into the initially proposed platform geometry. Their large 90x90 mm footprint physically clashed with the narrow 200 mm widening segments, making secure mounting impossible. Therefore, to accommodate these essential support structures, the platform dimensions had to be altered to a standardized size of 400x1000 mm. This iterative dimension change ensures the L-shapes can be securely implemented under every corner without protruding. An added benefit of this modular 40x100 cm standardization is that all platforms are now of equal size, which eliminates the need to place specific platforms in fixed positions, significantly reducing assembly complexity and setup time for the researcher.
The cost for this robust support solution is calculated to a total of €374.24.

11.2.5 Inter-frame connection

Each frame needs to be connected to the others to prevent the platforms from separating.
Several connector options are compared. The plate connector was chosen due to its low cost. It connects two items which are parallel to each other.
The bar connector was chosen for its ease of use. It connects two profiles by being slotted in the groove of each profile when is next to each other.
The bracket, due to its benefit of increasing structural stability, can connect the legs as well as the frames to the legs at the same time.
None of the explored solutions was allowed to drill into the existing frame to prevent a reduction in the structural strength of the frame; this is why the previously mentioned parallel connector is omitted as a choice. All these options can be seen in Table 17 in the *Appendix Cost analysis inter frame connectors*.

From the explored solutions, the plate connector is the cheapest by quite a significant margin. However, with this solution, a connector still needs to be chosen to connect the L-extrusions to the walkway since now only the legs are connected, the frame on top can still move in the xy plane.
This solution also brings additional cost and labour. Also, double connectors like the 90x90 can't be applied to the outside border of the walkway because it needs two profiles to mount it; however, on the edges, only one profile is available.
To determine the most cost-effective and structurally sound method for coupling the modular frames, a comparative analysis of the proposed solutions was conducted. The detailed breakdown of this comparison can be seen in Table 18 in the *Appendix Cost analysis inter frame connectors*.

Since the cost between the solutions is comparable and the structural capacity of the 90x90 bracket exceeds that of the 45x45 bracket significantly, it also reduces the number of different parts needed while also maintaining the same number of screws that need to be set to connect the walkway parts together. The choice was made to continue with the 45 brackets+90Brackets concept.

11.2.6 Length of the L extrusions

The final physical elevation of the walkway is strictly dictated by the required focal distance of the bottom-facing Intel RealSense D405 scanners to the top surface of the glass scanning plate. The physical housing of the D405 is 23 mm thick, and the required optimal focal distance to capture the plantar surface is 118.5 mm. Combined, this establishes a minimum total walkway height of 141.5 mm (from the clinical floor to the top of the walkway).
To determine the required length for the supporting L-extrusions (the legs of the frame), the physical thickness of the walkway structure itself must be subtracted from this total height. The current modular frames utilize 45x45 mm aluminium extrusions topped with a 15 mm composite surface plate (MDF and

vinyl), resulting in a structural thickness of 60 mm. Subtracting this 60 mm structure from the 141.5 mm total elevation results in an exact required leg length of 81.5 mm.

11.3 Scanner mounting

The current design of the printer has, as mentioned before, the scanner mounted directly connected to the walkway. This caused potential issues like the vibrations of the patient walking on the platform to carry through to the scanner. And would consequently influence the quality of the scan.
In the new design, an isolated support structure is designed for the scanner. The scanner frame will be made from 3030 extrusions since this provides ample strength as well as allows for several kinds of connecting supports to be used. Additionally, such an system allow for swapping parts out if needed, to account for a different scanner set-up in the future.
The use of extrusion also allows for the mounting of additional items like cable guides to prevent things from getting caught on the cable, as well as to clean up the design.

11.3.1 Farzam camera positioning

As mentioned in chapter 6.2, the position of the cameras and their overlap of the view has a significant influence on the accuracy of the scan. For the new scanner, these positions will be used. The positions are repeated in Table 5.

Table 5 - Final Camera Coordinates in cm for the scanner setup

	Cam 1	*Cam 2*	*Cam 3*	*Cam 4*	*Cam 5*	*Cam 6*	*Bottom*
X	28	-22	-65	-55	25	63	0
Y	48	43	30	-50	-43	-30	0
Z	26	25	23	26	17	17	-45

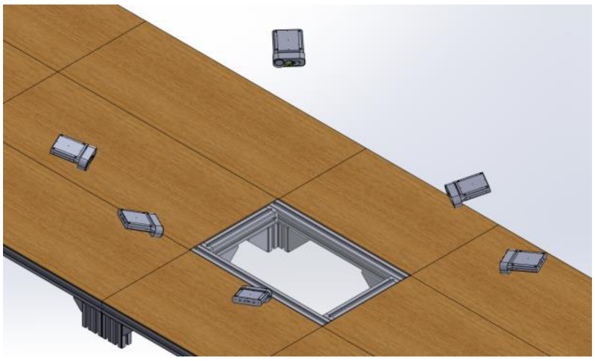

Figure 21 - Situation impression of the floating scanners

Due to the needed positioning of the scanners, they will need to “float” over the walkway(Figure 21). This creates additional design considerations. For example, how to ensure the newly designed won't tip over due to the overhanging position, this problem will be discussed in 11.3.3.

Figure 22 - K&F Mount with tuning knobs (Kameramarkt, 2026)

11.3.2 Scanner mount

Mechanical quality and adjustments

In the design of Kwa, the mounts are made of 3d printed plastic ball joints. These are susceptible to creep due to the continuous force applied to them by the weight of the scanner itself. This is not preferred due to the precise nature of the scanner.
To ensure maximal rigidity while allowing for fine-tuned adjustments to the orientation of the scanner, which can be done manually, a K&F 3-way panoramic tripod mount was chosen (Figure 22). Several other options were compared. These options were more compact or allowed for fine-tuned adjustment; however, the cost increase wasn’t enough to justify

them as a choice.

The K&F 3-way has a metal construction that negates the potential effects of sagging through time compared to the solution of Kwa.
It has separate knobs with clearly labelled indicators for the angle of the pitch/yaw and roll of the scanner. It allows the user to quickly get the scanner in roughly the right position and do the final adjustments gradually and precisely with the knobs. This way of adjustment is preferred due to the mobile nature of the scanner and thus its need for repeated dis- and assembly. The mount can hold 5 kg; the Femto bolt only weighs 335 gr so this won't pose an issue.

Cost
The cost of implementation at 959,94 is high; the cost is warranted due to the reduction in complexity of the set-up and the needed time for accurate set-up, and increases the fidelity of the scan due to its accurate set-up.

Figure 23 - Proposed Cheese plate (Smallrig Official, 2026)

Mounting
To be able to mount the mount to the extrusion, an interface is needed due to the fact that the mount has 3/8''mount whereas the connection of the extrusion can only be done by M6 screws.
To make this connection possible, an interface plate is used.
This interface plate is called a cheese plate in photography and cinematography. It is a metal slab filled with spaced holes in various common threadings to allow different threads to be connected to another (Figure 23).
The cheese plate is connected to the extrusion by M6 bolts with washers, so the difference in thread size won't pose a problem. It also allows for the mounting force to be evenly distributed to ensure a strong connection. After this is done, the mount can be screwed into the cheese plate. These come at a cost of 52,54 total.

Calibration
Even though the scanner will be placed as close to the ideal angle and position, a final software calibration will still be necessary to ensure the highest possible scan. The added accuracy due to positioning will, however, help with increasing the fidelity as the closed-loop algorithm proposed by Kwa benefits from this. It allows the algorithm to converge more rapidly and with higher accuracy, and thus provides a better scan.

11.3.3 Scanner mounting of the horizontal extrusion to the vertically mounted stand

In the new design, as mentioned previously and shown in Figure 21, the camera will need to be suspended above the walkway. To verify any potential solution, a force analysis needs to be done.

Force analysis
The scanner weighs 0,335 kg, the camera stand weighs 0,81kg and the cheese plate is estimated at 0,08 and together 1,23 kg. Due to the suspended design, a moment will also be applied to any potential solution. Depending on the position of the camera, the stands are placed as close as possible to the walkway; however, sometimes the stands need to be placed further away due to conflicting geometry with the legs Figure 24.

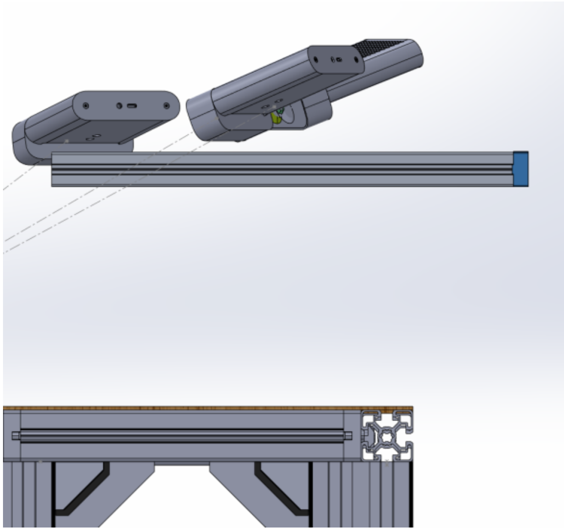

Figure 24 - Current situation of the scanner mounting system. With blue, the joint is indicated for which a possible solution is sought.

To find the moment of each camera, a table was made, and all relevant forces were calculated for each position. The assumption was made that all the connection where done with a straight connection from the stand. The applied force downwards was 12.3 N. A safety factor of 2 was applied. The highest found moment was 12Nm. All the results of the analysis can be found in Table 19**Fout! Verwijzingsbron niet gevonden.**, *Appendix Moment and cost analysis for the connectors that hold the scanner assembly*.

A specification comparison of several joint options was done in 22.1.2 to find the minimal viable solution that would be suited for the scanner.

The inner angle can't maintain the needed loads, so it is eliminated. Between the bracket and the t-joint, the t-joint is easier in use when kept in mind that the platform needs to be repeatably dis and assembled. The t-joint can stay connected to the extrusion without creating an odd shape during transportation, which makes it easier to store and transport. It is also a slightly cheaper solution, which is also beneficial.
For these reasons, continuing forward with the implemented solution will be the t-joint.

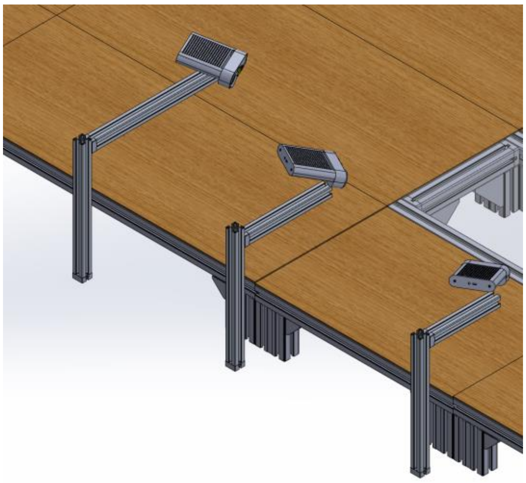

Figure 25 - Current Situation, an solution is sought to hold all the vertical supports stable

11.3.4 Scanner base

To ensure the scanners' positions can be held stable according to the requirements listed in chapter 8, a proper base needs to be designed.

Stability and tipping

Currently, the cameras are positioned above the walkway platform, as can be seen in Figure 25. Since no supports can be fixed to the platform itself due to the stated requirements (8.1.2), the supports need to be placed further away, as mentioned before. This creates an issue where the centre of gravity of the structure is far away from the base, which can cause tipping issues. To mitigate these issues, a stand needs to be provided for additional stability for the base against bumps and other potential issues.

All cameras on one side are connected by a central bar, as shown in Figure 26. Both bars are connected with two extrusions as shown in Figure 27. This ensures the centre of gravity stays underneath the platform and in front of each camera and thus prevents the structure from tipping over.
These bars and extrusions for the centre are too long to be transported in one piece. These bars are segmented into pieces and are connected by a profile lengthener.
The connecting extrusions that connect the bars are also the mounting point for the bottom camera. For this connection, once again, a t-joint is used since it can withstand the previous load, and this load is not significantly different since the vertical stand only presses on it and does not apply torque.

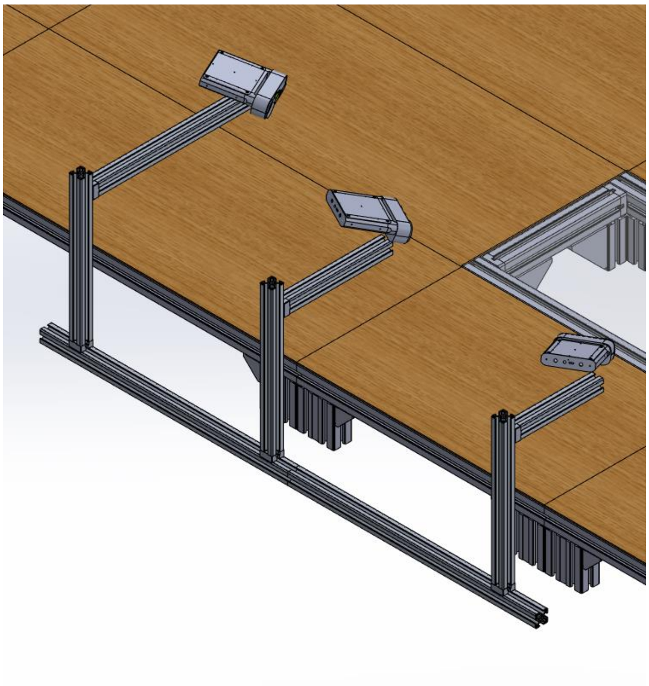

Figure 26 - Situation explanation of the use of the central bar

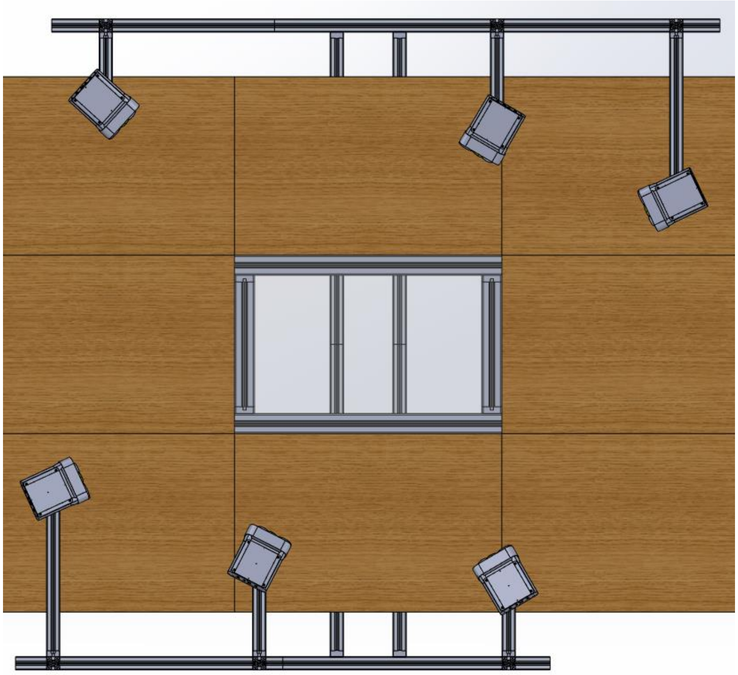

Figure 27 - Top Down view to show the final concept as well as the connecting bar for connecting both sides

By using a fixed mounting as this, it ensures that the relative positions are maintained, and that makes the amount of errors can be reduced (Kwa 2021).
Any accidental displacement of a camera would mean a new calibration needs to be run to avoid artefacts in the 3d reconstruction (Vidmar, 2020). By locking down this variable, it becomes more resistant to accidents and ensures high reliability and high-quality scans during clinical use.

In the table below, the final cost for this part of the scanner can be found. The parts that are indicated with (M) are parts that need to be machined on one end to accommodate the T-connector. This increases the cost by 1.00 euro due to additional machining costs. All extrusion prices are calculated in Table 6 from the prices provided by (Aluxprofile, 2026).

Table 6 - Cost calculation for the scanner stand

Camera Base			
Extrusions	**Amount**	**Individual cost**	**Total cost**
200(M)	2	2,90	5,80
250(M)	2	3,37	6,74
400(M)	2	4,80	9,60
500	3	4,75	14,25
600	2	5,69	11,38
700(M)	4	7,64	30,56
T connector	16	2,50	40
Profile lengthener	10	4,90	49
		Total	**167,33**

12 Final Concept Design

This chapter presents the final conceptual design of the redesigned 4D foot scanner. It serves as the culmination of the biomechanical, optical, and user-centric design explorations detailed in the previous chapters. By synthesizing these elements into one holistic system, this chapter demonstrates how the new architecture resolves the critical bottlenecks of the previous prototype to deliver a reliable, clinical-grade scanning environment.

12.1 Final design look

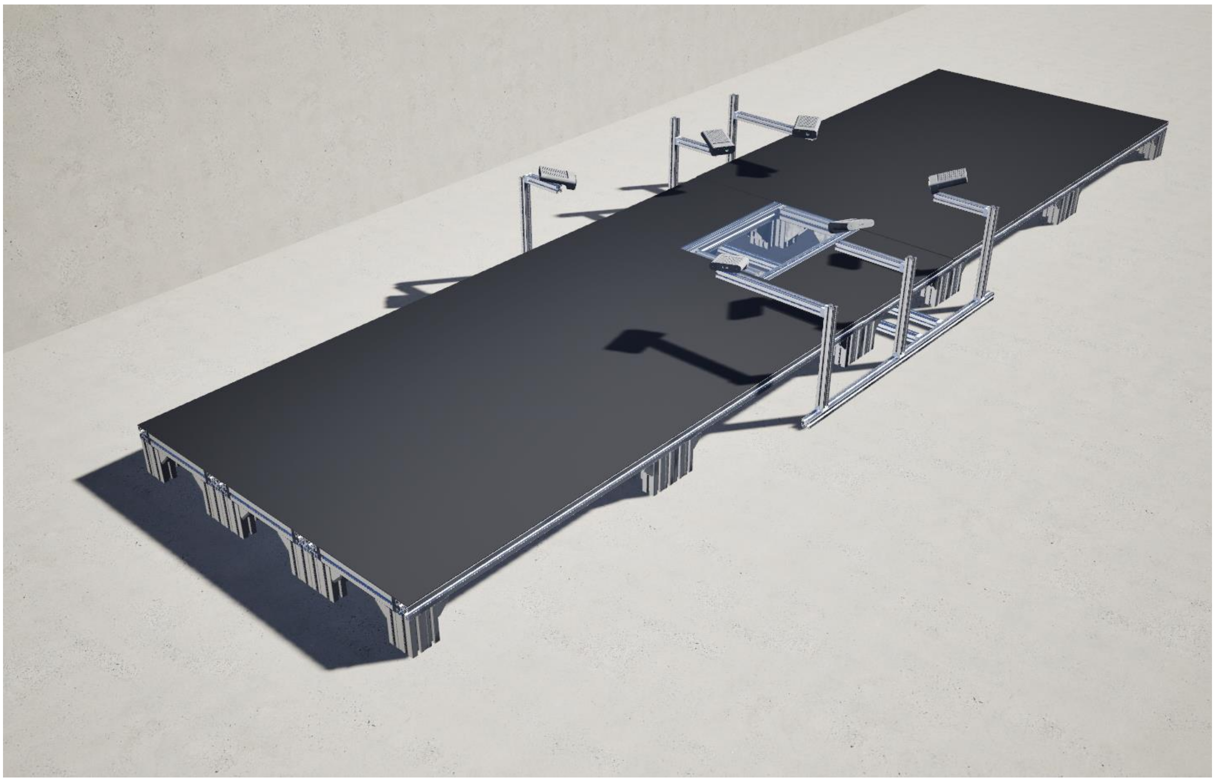

Figure 28 - Isometric view of the final design

The final conceptual design represents the successful integration of the mechanical and optical solutions explored during the project. As illustrated in Figure 28, the complete scanner assembly forms a continuous, low-profile walkway measuring 4.6 meters in length and 1.2 meters in width.
To completely eliminate the structural interference that plagued previous iterations, the design features a decoupled, 'floating' camera mounting system. The optical sensors are suspended from an independent 3030-extrusion frame that does not physically touch the walking platform, ensuring that step-induced cadence vibrations are no longer transferred to the cameras.
Furthermore, by transitioning to Intel RealSense D405 active stereo vision cameras for the bottom scanners, the required focal distance was drastically shortened. This allowed the physical step-up height of the walkway to be reduced to just 14.2 cm, effectively eliminating the need for an external step-up aid.

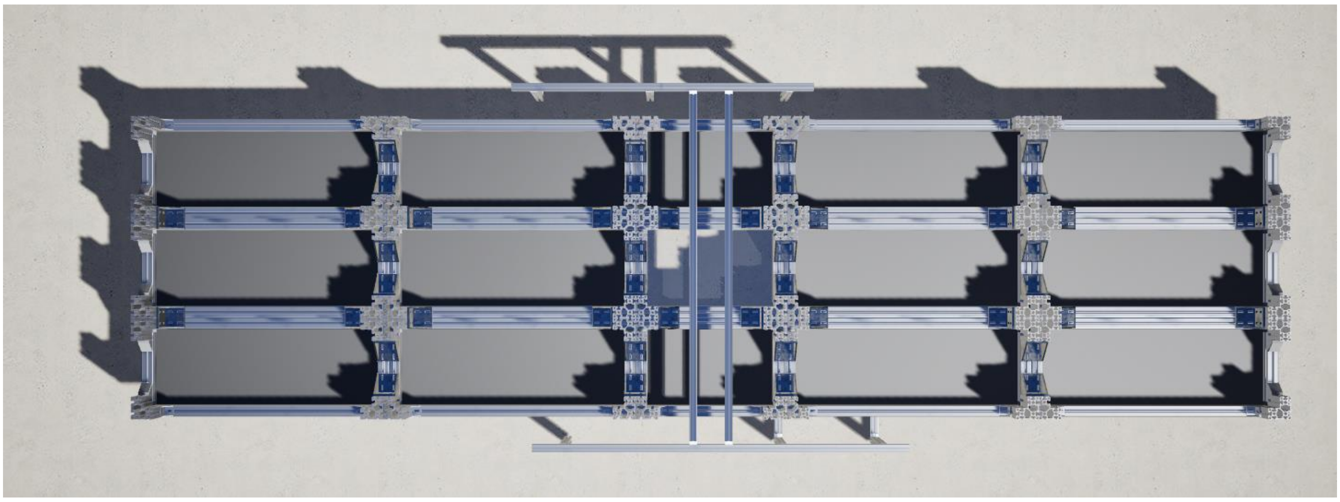

Figure 29 - Bottom view of the design

Underneath the surface (Figure 29), the walkway is supported by standardised 40x100 cm L-extrusion modules. These modular frames not only provide the structural rigidity required to withstand dynamic peak forces of 5200 N, but also allow the entire 4.5-meter setup to be rapidly disassembled for transport.

12.2 Improved User Workflow

Beyond meeting the technical hardware specifications, the final concept drastically improves the user journey for both the researcher and the patient (as previously outlined in Chapter 5).

12.2.1 For the patient

The most significant improvement is the reduction of perceived psychological distress. The VR studies demonstrated that both height and width play a crucial role in the fear of falling. By widening the walkway to 1.2 meters and lowering it to 14.2 cm, the design feels closer to a normal clinic floor. Combined with the textured vinyl surface and visual guiding lines, patients can walk with a higher degree of confidence, which is essential to capturing an unforced, natural gait.

12.2.2 For the researcher

The redesign heavily optimizes the setup and calibration phase. Because the walkway consists of interchangeable 40x100 cm modules with pre-attached L-extrusions, the assembly time is significantly reduced. Furthermore, the newly designed rigid T-joint camera mounts and the pre-calculated Farzam spatial coordinates ensure that the cameras are positioned with maximum view overlap from the start, mitigating the frustrating and imprecise manual calibration process of the previous prototype.

12.3 Deep dive financial analysis physical design

If all parts are added together the final cost of the design can be found in table 7. These are the prices found on the date of writing this report, august 2026.

Table 7 - Final cost break down

Name of the part	Individual cost	Amount	Total
General Platform	58,39	12	700,62
Side platform scanner	48,80	2	97,59
Scan Platform	164,80	1	164,80

Legs and needed parts	-	1	741,87
All cameras	-	1	4.000,90
Camera mounting	-	1	168,78
Camera Support	-	1	167,33
Total Physical cost			6.048,89

With a total hardware and structural cost of €6.048,89, this redesigned prototype remains exceptionally cost-effective. As verified, it stays well below the established clinical viability threshold of €30,000 (Requirement 8.1.8). While the modern depth cameras themselves represent the largest financial investment (€3,587.95), the drastic reduction in structural materials—achieved by lowering the overall walkway height and choosing 4545 extrusions over 5050—has significantly reduced both the financial and environmental footprint of the physical frame. This low price point effectively removes the primary financial barrier for widespread commercial adoption in standard podiatry clinics.
While the physical hardware of the redesigned scanner totals €6.048,89 a complete clinical setup also requires a dedicated processing computer (as stipulated in the economic requirement in Section 8.1.8). However, because data processing, software integration, and the selection of internal PC components fall explicitly out of the scope of this hardware-focused project (Section 2.4), a new computer configuration was not actively developed.
For reference, the previous prototype iteration by Kwa (2021) utilized a processing desktop with a total component cost of approximately €1,243. Even if a modern, high-end commercial workstation (estimated between €2,000 and €3,000) is necessary to process the higher resolution data from the newly implemented Intel RealSense D405 cameras, the total system cost will remain well below €10,000. This comfortably satisfies the maximum economic viability threshold of €30,000, proving the physical redesign provides a highly cost-effective foundation for standard clinical implementation.

12.4 Requirements Verification

To validate the feasibility of the final concept, the design must be evaluated against the core requirements established in Chapter 8. The redesign successfully meets the vast majority of the clinical and technical constraints:

- **Vibration Isolation (Met):** The camera mounts are entirely structurally decoupled from the main walkway frame, preventing any transfer of the 5200 N peak forces to the optical sensors.
- **Resolution and Capture Speed (Met):** The integration of the Femto Bolt and Intel D405 sensors guarantees a capture rate of 30 fps at a sub-millimetre resolution, preventing motion blur during the gait cycle.
- **Cost & Economic Viability (Met):** The total component cost is €6.048,89, remaining well below the strict clinical viability threshold of €30,000.
- **Portability (Met):** All walkway modules are standardised to a maximum length of 100 cm, ensuring the fully disassembled scanner fits into the trunk of a compact car (e.g., Volkswagen Polo).
- **Clinic Integration & Accessibility (Met):** The total height of the walkway was minimised to 14.2 cm, ensuring easy access for mobility-impaired patients without requiring permanent floor modifications.
- **Walkway Length & Scan Area Size (Partially Met / Altered):** The initial requirements dictated a 5-meter walkway and an enlarged 445x255 mm scan area. However, strictly adhering to the 1-meter portability constraint forced a design trade-off, resulting in a 4.5-meter walkway and a slightly smaller scan plate. A detailed reflection and justification of these specific trade-offs are discussed in Chapter 13.3 (Failed requirements).

13 Discussion and reflection

13.1 Research critiques and improvements

13.1.1 Validity of the research participants used

The user research and physical experiments conducted in Chapters 6 and 7 utilised relatively small sample sizes (ranging from N=8 to N=17) consisting predominantly of healthy individuals between the ages of 20 and 30 with only a few exceeding that range. This demographic profile significantly contrasts with the intended clinical target group of the 4D foot scanner: orthopaedic and podiatric patients, who are generally older and frequently suffer from mobility impairments, balance issues, or conditions such as diabetic foot ulcerations.

This discrepancy raises valid questions regarding the direct generalizability of the experimental findings. Healthy young adults typically exhibit greater walking speeds, longer step lengths, and higher physical confidence than the elderly clinical demographic. However, rather than invalidating the design, evaluating the prototype against the biomechanics of this healthy group actually reinforces the safety and spatial parameters of the redesigned walkway.

Because the walkway was lengthened to 4.5 meters to accommodate the longer, unforced acceleration and deceleration phases of a healthy young adult, it mathematically provides more than enough uninterrupted space for the shorter, slower strides characteristic of elderly patients. Furthermore, the Virtual Reality experiments demonstrated that even young, physically capable participants subconsciously experienced psychological distress (a fear of falling) on elevated or narrow platforms. By redesigning the physical scanner to eliminate these specific barriers—widening the platform to 1.2 meters and drastically lowering the physical step-up height to just 14.2 cm—the design proactively neutralises hazards for the most vulnerable users.

Therefore, while the initial data was gathered from a healthy demographic, the resulting barrier-free architecture ensures that the scanner is optimally suited, highly accessible, and exceptionally safe for the clinical target group. Nevertheless, a future physical validation study involving actual mobility-impaired patients remains a recommended next step to definitively confirm these ergonomic assumptions.

13.1.2 Reality vs VR

During the Virtual Reality (VR) simulation study detailed in Chapter 7, a notable discrepancy between virtual and physical perception was identified. Participants anecdotally indicated that standing on a physical object (such as a table) with comparable dimensions induced significantly more psychological distress than the VR equivalent. This discrepancy highlights a valid limitation regarding the absolute validity of the quantitative distress scores derived from the simulation. Because the VR setup lacked full-body tracking (meaning participants could not physically see their own feet), immersion was reduced. This absence of a physical consequence and visual body awareness likely led participants to underestimate their true level of discomfort.

Consequently, the minimum safety dimensions derived purely from the VR environment might still be insufficient to eliminate a "fear of falling" in a real-world clinical setting. To bridge this methodological gap in future research, a follow-up study incorporating full-body kinematic tracking is highly recommended. Providing participants with a 1:1 visual representation of their lower extremities in the virtual space would drastically increase immersion, likely yielding more accurate and directly translatable distress values.

Nevertheless, this limitation does not invalidate the core findings of the experiment or the resulting hardware decisions. The fact that participants consistently reported measurable discomfort even within this 'muted' virtual environment strongly confirms the underlying hypothesis: elevated and narrow walkways inherently disrupt a patient's sense of safety. Rather than discarding the data, this underestimation serves as a powerful justification for the highly conservative approach taken in the final design. Because the distress in reality is expected to be worse than in VR, the physical redesign deliberately overcompensates by maximizing the walkway width to 1.2 meters and minimizing the physical step-up height to a mere 14.2 cm. By aggressively mitigating these dimensions, the design ensures that even the most vulnerable patients feel entirely secure, which remains the fundamental prerequisite for capturing an unforced, natural gait cycle.

13.2 Failed requirements

Out of the 18 established requirements, four were not fully met in the final conceptual design. However, these deviations are heavily interconnected and stem from a single chain of design trade-offs, primarily driven by the strict portability requirement.

13.2.1 Walkway requirements

The first unmet requirements pertain to the 5-meter walkway length and the 60x60 cm central scanning area. To satisfy the strict 1-meter portability constraint, the walkway was standardized into 40x100 cm modular platforms. Achieving exactly 5 meters with these modules would necessitate custom-sized segments, increasing the total assembly by 16 additional components. To prevent excessive setup complexity for the researcher, the walkway was deliberately capped at 4.5 meters. This is a highly acceptable trade-off; gait research (Chapter 7) showed no statistically significant difference in gait alteration between a 5m and 7.3m baseline ($p = 0.071$), indicating that a 4.5m length remains clinically viable for capturing a natural stride.

Consequently, this modular 40 cm width standardization required narrowing Kwa's (2021) originally validated 60x60 cm glass scanning plate to 40x60 cm to ensure a seamless physical connection. While Kwa validated the original 60x60 cm design to safely withstand 5200 N peak dynamic forces, this geometric alteration voids that specific safety guarantee. Therefore, successfully optimizing the scanner's portability and assembly time introduces the necessary consequence of mechanically re-validating the new 40x60 cm glass platform before physical clinical implementation.

13.2.2 Scanner requirement

The second unmet requirement pertains to the raw resolution. The initial baseline dictated that the new hardware should exceed the Intel D435i's resolution of 848 x 480 pixels. However, the selected Femto Bolt (in NFOV mode) operates at 640 x 576 pixels.

This numerical deviation is a justified trade-off. As established in Chapter 9, raw pixel count does not solely determine 3D fidelity. The Femto Bolt's Time-of-Flight (ToF) technology offers superior edge quality and significantly less noise at a 75 cm distance compared to the D435i. Furthermore, the integration of two short-range Intel D405 scanners directly beneath the foot heavily compensates for this, achieving true sub-millimeter precision at the most critical scanning area. Thus, the overarching goal of a higher-fidelity scan is successfully met through superior sensor technology rather than a strictly higher pixel count.

13.2.3 Mount requirements

The third unmet requirement concerns mechanical precision. The initial baseline demanded that the mounts facilitate manual camera alignment within exactly 1 degree. While the newly implemented K&F 3-Way Tripod Heads drastically improve vibrational stability compared to previous 3D-printed joints, achieving an exact 1-degree mechanical alignment proved unfeasible with standard off-the-shelf components.

Meeting this strict requirement would necessitate the use of expensive industrial robotic micro-adjusters, which would cause the system to drastically exceed the €30,000 budget constraint. However, this mechanical deviation is highly acceptable as it is mitigated by software. The new mounts provide a rigidly stable baseline close to the optimal Farzam coordinates. From this stable physical position, the closed-loop software calibration algorithm can efficiently converge to the necessary accuracy. Failing this strict mechanical requirement was therefore an essential compromise to maintain economic viability without sacrificing final system accuracy.

13.3 Future recommendations

13.3.1 Prototype Construction and Biomechanical Validation

As the current iteration of the redesigned walkway remains a theoretical concept, the immediate next step for future research is the physical construction and empirical validation of a functional prototype. This validation must encompass both mechanical integrity and biomechanical effectiveness. Specifically, in-vivo testing with the actual clinical demographic (patients with mobility impairments) is required to verify if the lowered step-up height (14.2 cm) and the 4.5-meter walkway length successfully facilitate a natural, unforced gait compared to the previous prototype. Furthermore, a critical mechanical safety test must be executed. Because the central glass scanning plate was resized to 40x60 cm to accommodate the new modular architecture, it must be practically re-validated to guarantee it can safely withstand the 5200 N dynamic peak forces before any human trials commence.

13.3.2 Hybrid Software Integration and Calibration

Beyond the physical structure, significant software development is required to realize the new hybrid scanning architecture. The deliberate choice to combine the Femto Bolt (Time-of-Flight) with the Intel RealSense D405 (Active Stereo Vision) presents a highly complex technical challenge, as it requires merging two fundamentally different sensor ecosystems. A custom software pipeline must be written to interface with both proprietary APIs simultaneously. A critical hurdle within this development will be achieving microsecond-precise hardware synchronisation—ensuring that the hardware triggering signals fire concurrently across both systems—to prevent temporal mismatch during the dynamic 4D capture. Additionally, a unified closed-loop calibration algorithm must be developed to accurately map the distinct point clouds from these different sensor types into a single, cohesive global coordinate system.

13.4.3 Re-calculation of Spatial Coordinates (Farzam Algorithm)

The optimal camera coordinates calculated in Chapter 5, utilizing the Farzam optimization algorithm, were specifically tailored to the intrinsic parameters of the baseline Intel RealSense D435i. Although the final conceptual design successfully upgrades the hardware to the Femto Bolt and Intel D405 to improve resolution and reduce the physical walkway height, these new sensors possess fundamentally different focal lengths and Fields of View (FOV).

Because of these differing specifications, the currently calculated spatial coordinates will not provide the exact mathematical maximum view overlap for the new hardware configuration. Therefore, a crucial recommendation before constructing the physical prototype is to re-run the Farzam optimization algorithm. By inputting the specific optical parameters of the newly selected cameras, a new set of optimal coordinates can be generated, ensuring that the final hybrid camera network achieves maximum 3D scanning fidelity without any blind spots.

13.4.4 Rapid Technological Advancements and Emerging Hardware (e.g., D585)

Because this design and research project spanned several years, the landscape of depth-sensing technology has evolved rapidly during its execution. While the current redesign effectively integrates the modern Femto Bolt and Intel D405 sensors to solve the immediate bottlenecks of the previous prototype, newer depth cameras continue to enter the market at a fast pace.

For instance, the recently emerged Intel RealSense D585 (or equivalent new-generation close-range sensors) offers highly optimized close-range depth sensing with an effective range around 40 cm. This specific technology could potentially be an even better fit for the bottom-facing scanners than the currently proposed setup. For future iterations of the 4D foot scanner, it is highly recommended to continuously evaluate such newly emerging hardware. Adopting these continuous technological advancements could further simplify the system architecture, reduce the need for complex hybrid software integration, and continuously enhance the sub-millimeter accuracy of the dynamic scans.

14 Bibliography

Aetrex Worldwide, I. (2021). *The Ultimate All-in-One Foot Scanning Solution.* Technical Specifications & Whitepaper.

AluProfilTechnik. (2026, 2 4). *Verbindungsplatte 45x 90 schwarz Pulverbeschichtet mit Befestigung für Profil 45 Nut10 B*. Retrieved from AluProfilTechnik: https://www.alu-profil-technik.de/Verbindungsplatte-45x-90-schwarz-Pulverbeschichtet-mit-Befestigung-fuer-Profil-45-Nut10-B.html

Aluxprofile. (2026, 01 25). *Aluminium constructieprofiel 4545*. Retrieved from Aluxprofile.nl: https://www.aluxprofiel.nl/aluminium-constructieprofiel-4545/a4191?filter=98&m=4390

Aluxprofile. (2026, 2 3). *Aluminium slot profile 3030*. Retrieved from aluxprofile: https://www.aluxprofile.com/aluminium-slot-profile-3030/a3661?filter=41

Arnaldo, L.-J., & Anselmo, F.-N. (2022,). Chapter 3 - Gait analysis: overview, trends, and challenges. In *Optical Fiber Sensors for the Next Generation of Rehabilitation Robotics* (pp. 53-64). Academic Press.

AYX Garden Supplier Store. (2026, 1 29). *2 Gaten Aansluiten Plaat Aluminium Fittings 2020/3030/4040/4545 Aansluiten Plaat*. Retrieved from Aliexpress: https://nl.aliexpress.com/item/1005001856433276.html?gatewayAdapt=glo2nld

Barr, L. R. (2025). *To scan or not to scan? Comparing the effectiveness and cost differential of insoles manufactured from foam-box casts versus direct scans in treating musculoskeletal conditions of the foot and ankle: a double-blinded, randomised controlled trial.* doi:https://doi.org/10.1186/s12891-025-08513-2

Barreto, M. A., Perez-Gonzalez, J., Herr, H. M., & Huegel, J. C. (2022). *ARACAM: A RGB-D Multi-View Photogrammetry System for Lower Limb 3D Reconstruction Applications.* Sensors. doi:https://doi.org/10.3390/s22072443

Barreto, M. A., Perez-Gonzalez, J., Herr, H. M., & Huegel, J. C. (2022). *ARACAM: A RGB-D Multi-View Photogrammetry System for Lower Limb 3D Reconstruction Applications.* Sensors. doi:https://doi.org/10.3390/s22072443

Boppana, A. &. (2021). *Dynamic foot morphology explained through 4D scanning and shape modeling.* Journal of biomechanics,. doi:https://doi.org/10.1016/j.jbiomech.2021.110465

Çağatay, B. E., Emre, S., & Seda, K. (2022). *CNN-based severity prediction of neurodegenerative diseases using gait data.* Digital Health.

Corporation, I. (2022). *Intel RealSense D405 Datasheet.*

D.A. Winter. (2009). *Biomechanics and motor control of human movement.*

G. Kontogianni, A. T. (2018). *Exploting mirrors in 3D construction of small artifacts.* Athens.

Grunnet-Jepsen, A., Winer, P., Takagi, A., Sweetser, J., Zhao, K., Khoung, T., . . . Woodfill, J. (n.d.). *Using the RealSense D4xx Depth Sensors in Multi-Camera Configurations.* Intel.

Hansard, M. L. (2012). *ime-of-Flight Cameras: Principles, Methods and Applications,.* SpringerBriefs in Computer Science.

Intel. (2026). *RealSense Product Family Datasheet.*

Kameramarkt. (2026, 4 25). *K&F 3-Way Panoramic Tripod Head*. Retrieved from Kameramarkt: https://www.kameramarkt.nl/k-f-3-way-panoramic-tripod-head?gad_source=1&gad_campaignid=20976546951&gbraid=0AAAADrF8mvjHPZrjhzQs9IPEuRW2aARA&gclid=Cj0KCQjw7IjOBhDyARIsAFzrWQy4uKm1pKhlWTkdIjdc87H3Sd2orLpo26MTGJl04FUO6BoIsaqtPiQaAtNJEALw_wcB

Kumar, P. (2024). Time-of-Flight (ToF) Cameras vs. other 3D Depth Mapping Cameras. *E-con Systems*.

Kwa, F. (2021). *Design of an accurate and low cost 4D foot scanner for podiatrists.*

Lee, Y. L. (2014). *Comparing 3D foot scanning with conventional measurement methods.* doi:https://doi.org/10.1186/s13047-014-0044-7

Mobbs, L., Fernando, V., Fonseka, R. D., Natarajan, P., Maharaj, M., & Mobbs, R. J. (2025, 1 20). *Normative Database of Spatiotemporal Gait Metrics Across Age Groups: An Observational Case–Control Study.* Sensors. doi:https://doi.org/10.3390/s25020581

Orbbec Inc. (2023). *Femto Bolt Datasheet V1.0.*

Rexroth. (2019). *Basic Mechanic Elements.*

Richard W. Bohannon, A. W. (2011). *Normal walking speed: a descriptive meta-analysis.* Physiotherapy.

RS-online. (2026, 1 29). *Bosch Rexroth M5mm Parallel Connector, Connecting Component, Strut Profile 8, Groove Size 8mm*. Retrieved from rs-online: https://nl.rs-online.com/web/p/connecting-components/2670634?cm_mmc=NL-PLA-DS3A-_-google-_-CSS_NL_NL_Pmax_1225-_--_-2670634&matchtype=&&gclsrc=aw.ds&gad_source=1&gad_campaignid=23353140411&gbraid=0AAAAADkeWNNO6o2w64acb9MYvM9B-BUmi&gclid=Cj0KCQiA4eHLBhCzAR

Sarbolandi, H. L. (2015). *Kinect Range Sensing: Structured Light versus Time-of-Flight.* Computer Vision and Image Understanding.

Sheng Yi Da Store. (2026, 1 29). *Europese standaard aluminium profiel éénlijns connector parallelle klemkop 4545 docking vast blok ingebouwde connector*. Retrieved from Aliexpress: https://www.aliexpress.com/p/tesla-landing/index.html?scenario=c_ppc_item_bridge&productId=1005005250931085&_immersiveMode=true&withMainCard=true&src=google&aff_platform=true&isdl=y&src=google&albch=shopping&acnt=272-267-0231&isdl=y&slnk=&plac=&mtctp=&alb

Shi, A. &. (2016). *Automatic foot scanning and measurement based on multiple RGB-depth cameras.* Textile Research Journal.

Silva, R. S. (2024). *A Review on 3D Scanners Studies for Producing Customized Orthoses.* Sensors. doi:https://doi.org/10.3390/s24051373

Smallrig Official, S. (2026, 4 25). *SmallRig Video Switching Kaasplaat Camera Eenvoudige plaat voor railblokken, zwaluwstaarten en korte staven voor DSLR-camerakooi Rig 1598*. Retrieved from Aliexpress: https://www.aliexpress.com/p/tesla-landing/index.html?scenario=c_ppc_item_bridge&productId=32721628300&_immersiveMode=true&withMainCard=true&src=google-language&aff_platform=true&isdl=y&src=google&albch=shopping&acnt=272-267-0231&isdl=y&slnk=&plac=&mtctp=

Tajdari, F., Eijck, C., Kwa, F., Versteegh, C., Huysmans, T., & Song, Y. (2022). *Optimal position of cameras design in a 4d foot scanner.* HAL open science. Retrieved from https://hal.science/hal-03685573v1

Thabet, A. K., Trucco, E., Salvi, J., Wang, W., & Abboud, R. J. (2014). *Dynamic 3D shape of the plantar surface of the foot using coded structured light: a technical report.* doi:https://doi.org/10.1186/1757-1146-7-5

Thomaidis, A. (2014). *Scanning with Mirrors.*

Tölgyessy, M. D. (2021). *Evaluation of the Azure Kinect and Its Comparison to Kinect V1 and Kinect V2.* Sensors.

Williams, B. D. (2020). *Is Scanning More Effective Than Casting For Custom Orthoses?* Podiatry Today.

Xu, J. e. (2018). *rapping Light for Time of Flight: Surround 3D Scanning using Light Traps.* IEEE Conference on Computer Vision and Pattern Recognition (CVPR).

Zhang, L. Y. (2023). *An exploratory study of dynamic foot shape measurements with 4D scanning system.* Sci Rep. doi:https://doi.org/10.1038/s41598-023-35822-0

15 Appendix: Aligning participants' steps with the scan area experiment 1

15.1 Introduction

For the most efficient use of the scanner, an appropriate camera position has to be calculated. However, currently, the assumption has been made that the user will align their foot with the middle of the platform. Indicate with the green foot.

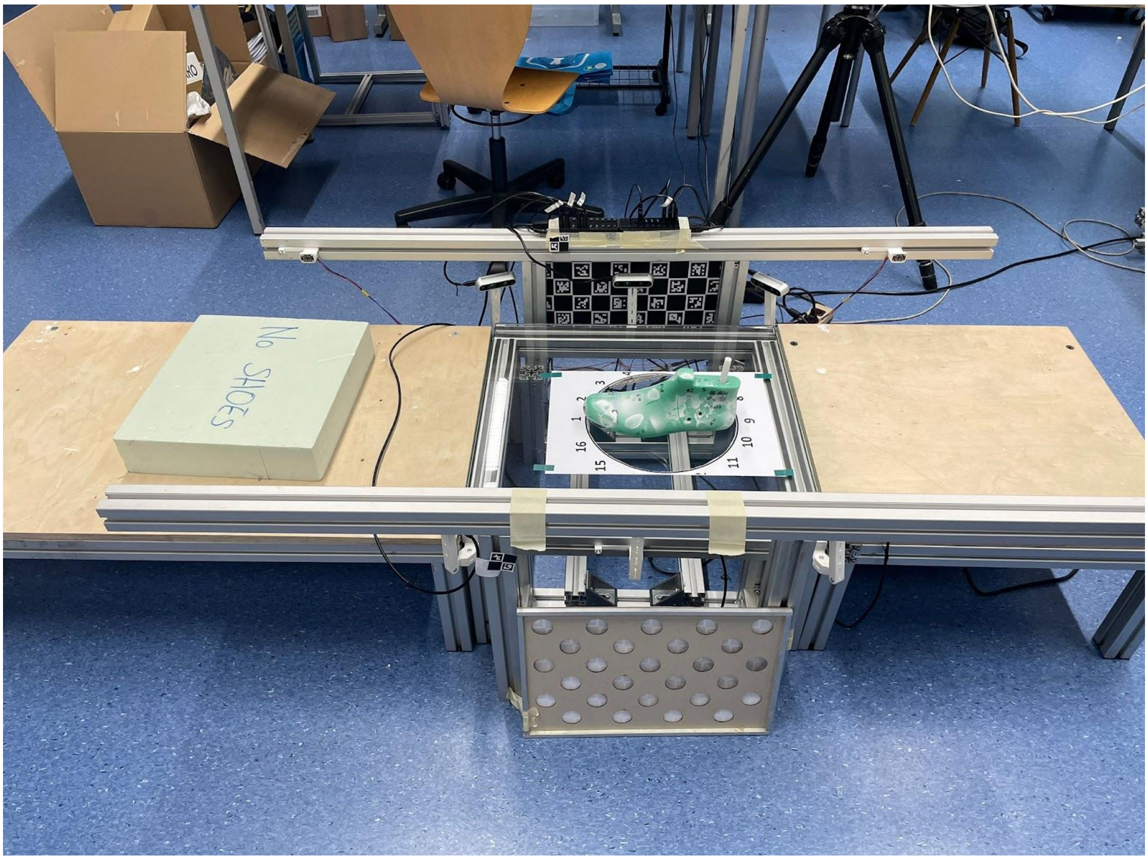

Image 1: Current design of the foot scanner.

However, this is an assumption to further advance the use of the scanner it is needed to analyse where users are currently putting their foot down. And if it is possible to guide users to step in the middle with certain methods of guiding them.

15.2 Set-Up

The 3 walkways (brown) were separated by a resting area (red) with a stool (blue circle) where the participants could sit and their feet got repainted. The placed stool also allowed the researcher to position the foot of the subject in the proper place when this was needed. at the end of the walkway is a tub (blue square) where the participants could wash their feet.
Figure 1 shows down below the rough layout of the entire setup.

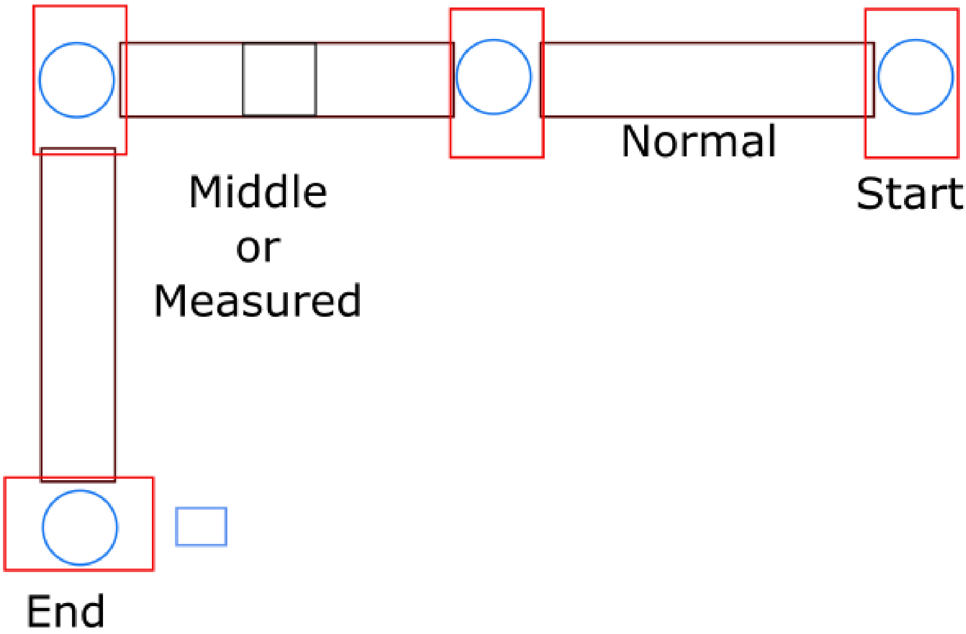

Figure 1: Set-up of experiment

15.3 Method

To validate where users place their feet on the scanner an experiment was done. The experiment was done with 8 participants (3 females and 5 males), 6 within the age range of 20 and 30, 2 around 60 years, with a varying height between 1.6m and 2.1 and BMI between 21 and 28,7.

Several measurements were taken to quantify to wide differences of the participants of our study.
The height, hip-width, stature and weight of the test subject were asked or measured. As well it was asked with which foot they would kick a ball.
To ascertain the current step length to see if there is any variation in step length due to the use of paint. The participants were instructed to walk between 2 lines spaced at a 3m distance several times while counting the steps that were taken. The total distance is divided by the taken steps to come to the test subjects step length.
The subjects have their feet painted, step on the paper walkway and then walked normally across a sheet of paper with a length of 2.6m to ascertain if the step length changes due to the length of the walkway. Also, this produced a heat map of where the participants walked on the platform without any instructions.
The participant has their feet painted, step on the paper walkway, where they were asked to and then try to align their feet in the middle of a 600mm square that was marked on the 2.6m paper walkway.
This was done to verify if the step length changes due to the instructions given. It also produced a heatmap of the steps taken by the test subject on the scan platform.

After which their step length is looked up and used to determine their starting position. By the use of the following formula:

Steps to the middle of the platform = Distance to the half of the platform / Steplength
The number that follows is almost always a whole number with some decimals.

Distance to compensate = decimals * steplength
This gives the distance to compensate so the heelstrike is in the middle of the platform.

At random, the decision will be made to ask the participant to try to align their foot right or left foot with the middle of the platform. The participants will be moved accordingly so the scanned foot is aligned with the middle. Also if the user needs to hit the middle of the scan area with their non-dominant foot the start will be moved one step length backwards. These steps are taken to ensure that the test subjects align their step as natural as possible with the middle of the scanning area.
The participant has their feet painted, step on the paper walkway and were given the assignment to cross to the other side.

Here the goal is to ascertain if it is possible to let the test subjects step closer to the goal. This can be verified by comparing the 3 heatmaps and to see which produces to tightest heatmaps.
The walkway where the subjects steps in the middle and the one where the subject starts at a calculated position will be switched to prevent the carryover effect where the subject already gets accustomed to one task, or by consequently testing in one order certain results may be skewed.

15.4 Result

After the experiment was completed all walkways were measured and were digitized by measuring each heel strike location, foot length and width. After this, each step was drawn with the given coordinates in a digital drawing program.

It was noted that 6 out of the 8 were taking smaller steps with paint compared to the measurement without paint. However, after each walkway, the step size increased for most participants.

Table 1: difference in step length in percentages

Difference step length per participant	1	2	3	4	5	6	7	8	Average Difference step length
Normal	-18,10	1,67	-5,38	-13,37	-16,22	-8,21	6,50	-17,42	-8,82
Middle	-17,02	-8,33	7,60	-2,37	2,22	-0,42	13,25	-12,58	-2,21
Measured	-13,15	-18,33	8,98	-9,53	4,71	5,13	18,90	6,13	0,35

This produced the following figures(2 and 3).

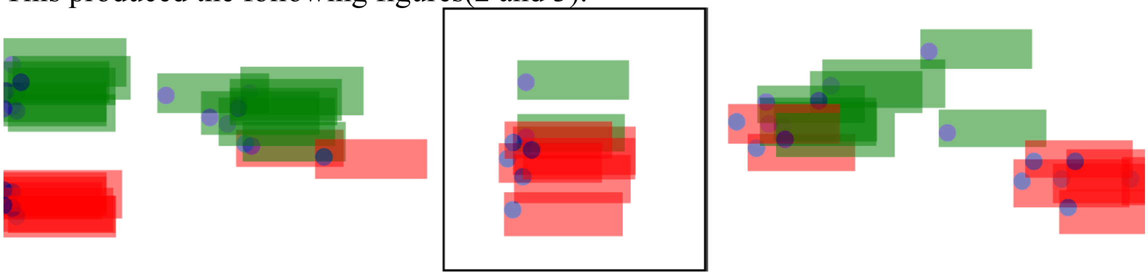

Figure 2: Overlay footsteps with the assignment to put their foot in the middle. The green square is the left foot, the red square is the right foot and the blue dot indicates the heel strike.

Figure 2 shows how the participants walked when given to place their right or left foot in the middle of the scanning area, indicated here by the use of the black square.
As can be seen, 5 placed their feet reasonably in the centre and 3 diverged more towards the outside.
It was observed that during this assignment all participants were struggling with deciding which foot to place first to ensure that they would land with the proper foot in the middle. All participants were looking down to the ground to see if they placed their foot correctly in the middle. For 4 of the 8, the step to align with the middle was the biggest they took. Also, it can be seen, that the participants have only taken one step before placing the foot to be scanned on the scanner. This far before the participant has reached their natural walking cadence.

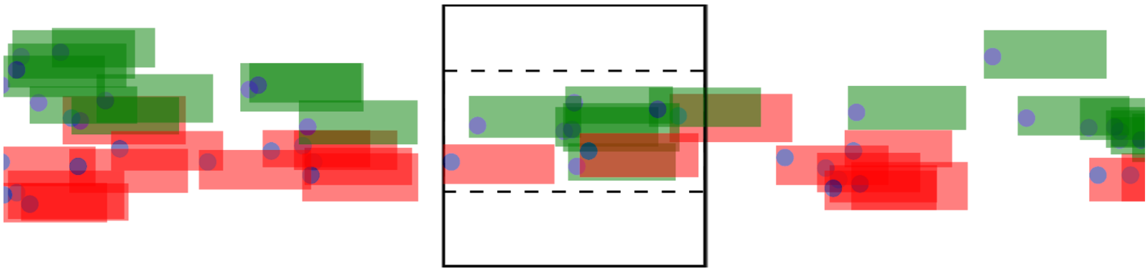

Figure 3: Overlay footsteps with the assignment to walk across. The green square is the left foot, the red square is the right foot and the blue dot indicates the heel strike.

Figure 3 displays the footsteps of the participants when their step length was measured and compensated beforehand by placing one foot in the front of the other. As can be seen, here the steps are closer together. None of the participants was looking at the ground and was walking more natural.

15.5 Discussion

15.5.1 Influence of the instruction and foot placement

When comparing methods 2 and 3 it can be seen that just commanding the participants to place their feet in the middle of the square, does not allow for a natural walk. This can be seen that the participant already struggle to think with what foot to start and during their walk keeps looking down. As well as their step size where the step that lands in the middle of the platform is bigger than usual.
When the starting position of the feet was given a more natural walking pattern emerged. The participant walked without looking down and the step sizes were more consistent.

15.5.2 Formula

The formula seems to be working. It tightens the positions of the foot in the vertical direction as well allow for a more natural gait.
However, the alignment is not ideal. This is since the formula the calculate the position of the foot did not account for the foot length of the participant but only for the heel strike. Currently, it is as follows:

Steps to the middle of the platform = Distance to the half of the platform / Steplength

The number that follows is almost always a whole number with some decimals.

Distance to compensate = decimals * steplength

This gives the distance to compensate so the heelstrike is in the middle of the platform however the whole needs to be scanned so the formula should be this:

Distance to compensate = decimals * steplength * 0.5 * footlength

This would ensure the foot is properly in the middle of the platform.

15.5.3 Length of the walkway

The current walkway is too short.
Almost all participants only needed 4 steps to come to the end of the walkway.
For 1 participant with a steplength of 70 cm, his first step would be the step that needs to be scanned and with the second step, he already was at the end of the walkway.
This distance is too short for the participant to reach a stable walking rhythm. So the walkway before the scan platform should be lengthened to accommodate this.
Most of the participants were still increasing their step length which levelled off during their fourth step (probably due to reaching the edge o the walkway). To ensure a subject has reached their normal step length it is advised to add 3 steps before the foot that needs to be scanned is placed down.
To ensure that even tall people will be able to do so the walkway needs to be 2.85m before the participants place their foot down (3*70cm +20cm for the distance to the edge +35 cm to ensure the step lands in the middle of the platform)

15.5.4 Interaction with the walkway

During the experiment, it was observed that all people increased their average steplength in their second run. This is probably due to getting familiar with the sensation of paint under their feet.

15.5.5 Placing the foot in the calculated position

Placing the foot upon the calculated position was cumbersome for the participant as well as the researcher. The spot where the foot needed to be placed needed to be marked and measured with tape measures. This process could be eased by using a grid-like system where it is visible where the foot needs to be placed.

16 Appendix: Aligning participants' steps with the scan area experiment 2

16.1 Introduction

From the previous experiment, several questions arose regarding the potential impact of walkway length on individuals' step lengths, and subsequently, its influence on the accuracy for natural walking gaits of the scans. To investigate these effects, the following hypotheses were formulated:

From the previous experiment it was observed that participants would reduce their final step length to stay on the walkway when reaching the it’s end. This change in step length could indicate a change in the walking gait as a whole and this needs to be prevented if the goal is to capture the natural gait of an individual. To see if the walkway length has an effect on the step length the following hypothesis was formulated:

1. Due to the short length of the 3-meter walkway, it is expected to influence an individual's step lengths significantly.

Furthermore, in the previous experiment, the step length seemed to increase due to repeated walking on the same walkway. This effect could influence the results of a scan and would need to be accounted for if these scan are used to design inserts. To verify if this assumption was happening the following hypothesis as formulated:

2. Step length increases after repeated use of the walkway.

The current design of the scanner features a glass plate of 60*60 cm. For a potential redesign it was hypothesized that a smaller scan plate might make it easier for patients to align their feet to the middle of the plate.

3. The width of the glass plate is expected to have an impact on the proximity of participants' steps to the middle of the scan plate.

16.2 Set-up

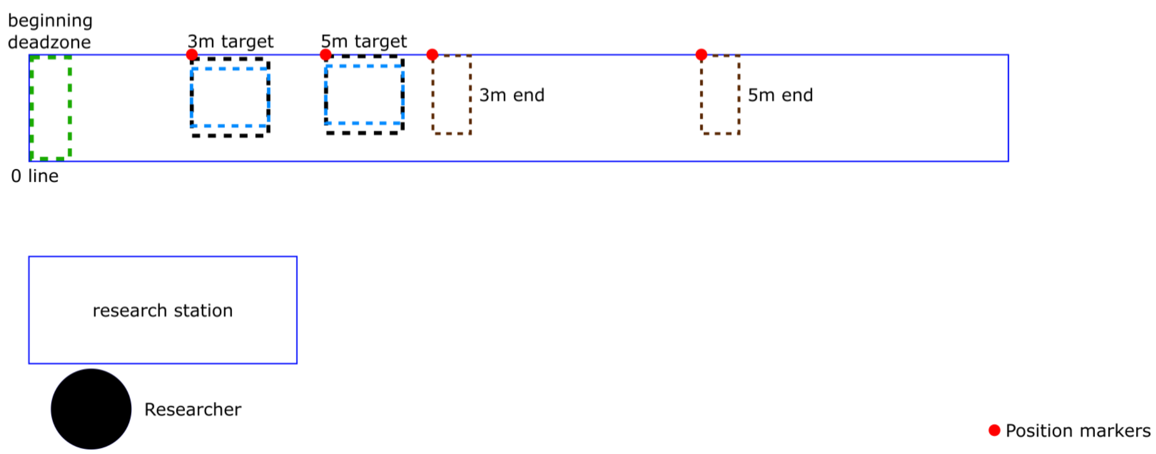

Figure 30 - Top view of the lay-out of the set-up

Figure 31 - Overview of the situation in practice

A Gaitrite walking mat was positioned, with a designated zero line aswell as as a line which designated the dead zone of the mat. For the researchers use of use, several reference points were marked on the mat from the zero point on the mat. These markers were placed at 1.2 meters, 2.2 meters, 3 meters, and 5 meters.
The first two markers were used for aligning and laying out the cloth, while the last two markers indicate the placement for a cardboard box which was used to signal the end of the walkway.
Adjacent to the walkway, a table was set up to allow for data recording via laptops and allow the experiment observers to sit and monitor the experiment.

16.3 Method

Numerous measurements were conducted to quantify the different characteristics among the participants in our study.
Anthropometric data, including weight, height, foot length, and foot width, were recorded for each participant.
To ascertain participants' dominant foot, they were requested to indicate which foot they would use to kick a football.
After this, the participants were instructed to walk over a 7-meter mat. This was done to acquire an baseline, where the participant was walking unobstructed.
Following this initial test, participants were asked to walk over either a 3-meter or 5-meter mat, both of which ended where participants were asked to step over an cardboard box before continuing with normal walking.
Afterwards, participants were tasked with walking over both a 3-meter or 5-meter mat and were asked to target the centre of a red cloth with their dominant foot, which represented the glass plate of the scanner. The cloth's width was varied between 45 and 60 centimetres, to be used as an representation for the resized of the glass plate.
To prevent any potential carryover effects, the order of cloth width and mat length combinations was randomized among participants.
Upon successfully hitting the designated target, participants were instructed to resume their normal walking pattern, eventually encountering the carboard box that required the participant to step over before continuing walking normally.
Upon reaching the end of the mat, participants were instructed to walk alongside it and position themselves within a designated "dead zone" to prepare for the subsequent trial.

16.4 Results

Hypothesis 1 and hypothesis 2
After this was done for each participant and for each patients run the steps were averaged and these were inputted into the two-way Anova analysis. The formula for the ANOVA analysis was as following:

$$Avarage\ steplength = run * length\ of\ the\ walkway$$

The results can be found in Table 8.

Table 8 – Repeated Measures ANOVA results

	F Value	Num DF	Den DF	Pr > F
Length of the walkway	7.1620	2	32	0.0027
Run	0.8189	2	32	0.4499
Length of the walkway: Run	2.2190	4	64.0000	0.0767

These results indicate a significant main effect of walkway length on the average step length (p = 0.003). However, this initial result does not specify which walkways significantly differ from the 7.3m baseline. To further analyze this, post-hoc paired t-tests with a Bonferroni correction were conducted. This analysis showed a significant difference between the 3m and 7.3m walkways (p = 0.005), but no significant difference between the 5m and 7.3m walkways (p = 0.071).

To quantify this impact, Cohen's d effect sizes were calculated. The comparison between the 3m and 7.3m walkways yielded a d = 0.85, indicating a large effect, with the average step length being reduced by 3.86 cm compared to the baseline. The 5m walkway demonstrated a moderate effect (d = 0.56) on the average step length, with a reduction of 2.17 cm.

The number of runs itself had no significant main effect on the step length (p = 0.450).

Furthermore, the interaction effect was not significant (p = 0.077), demonstrating that the patients' step length was not influenced by an interaction between the number of runs and the length of the walkway.

Hypothesis 3

The next analysis aimed to determine if the width of the mat influenced participants' proximity to their step goals which was the centre of the red cloth. An analysis was done to see if the length of the walkway and the width of the cloth had an influence on the proximity of the foot to the centre of the red cloth.

For the data the results were filtered to only include the steps of each run for each patient that was closest to the target. After this the centre of the foot was calculated by subtracting the locating of heel contact from the contact point of the toe.

With these found, an repeated measures ANOVA was done for each axis . The formulas were as following

$$distance\ X\ of\ target\ =\ length\ of\ walkway\ *\ size\ of\ the\ cloth$$

$$distance\ Y\ of\ target\ =\ length\ of\ walkway\ *\ size\ of\ the\ cloth$$

These gave the following results that can be seen in Table 9 and Table 10.

Table 9 - Result ANOVA for the x-axes

	F Value	Num DF	Den DF	Pr > F
Width of the cloth	1.0690	1	13	0.3200
Length of the walkway	0.6189	1	13	0.4456
Length of the walkway: Width of the cloth	2.0250	1	13	0.1783

Table 10 - Result ANOVA for the y-axes

	F Value	Num DF	Den DF	Pr > F
Width of the cloth	0.2956	1	13	0.5958
Length of the walkway	2.5457	1	13	0.1346
Length of the walkway: Width of the cloth	6.1146	1	13	0.0280

From this the conclusion can be drawn that neither the width of the scan platform nor the length of the walkway has an significant influence on the patients ability to place their foot in proximity of the centre of the target.
And the experiment results are visualized in Figure 14

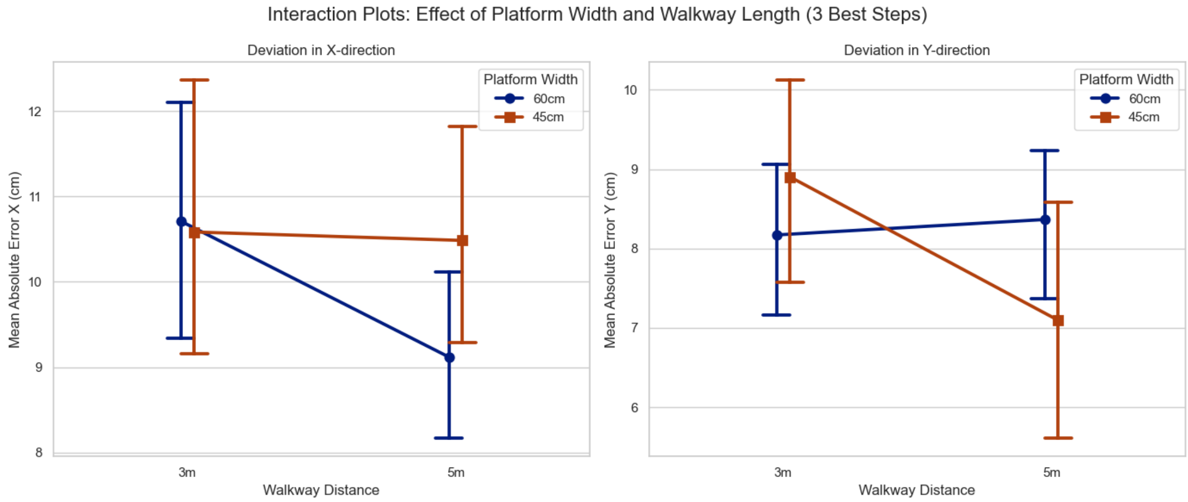

Figure 32 - interaction Plots: Effect of Platform Width and Walkway Length (3 Best Steps)

Additional Observations
Also an interesting observation was that all participants would look down during walking due to the assignment given. This could lead to a less natural gait, which in turn could influence results.

16.5 Discussion (discuss and possible recourse)

1. Hypothesis: Due to the short length of the 3-meter walkway, it is expected to influence an individuals' step lengths significantly.

Hypothesis 1 is confirmed by the result of the experiment. However this effect seems to lessen with the 5m walkway. This result seems to indicate that it is preferred to change the design of the walkway to one with a 5m one, so the participant has a more natural gait once they arrive at the designated area to scan their foot.

2. Hypothesis: Step length increases after repeated use of the walkway.

This hypothesis was shown to be false. This tells us that the first scan a patient does is just as valid as the 3rd which might reduce the time needed to capture a scan of a patient.

3. Hypothesis: The width of the glass plate is expected to have an impact on the proximity of participants' steps to the target.

From the experiment it was concluded that the width of the glass walkway doesn’t influence the proximity of the step to the target area however a follow-up study might be advised where the width of the cloth is further reduced to see if this would make it easier for the participant to line up their step.
Or to do a different study where the effectiveness of visual aids is tested to help align the participant's steps with the middle of the walkway for an optimal scan.

17 Appendix: The influence of the combined effects of height and width on perceived discomfort

17.1 Introduction

In the current walkway design, the platform is 30cm of the ground and 60cm wide, however, these measurements of the heights and widths might influence the gait of potential patients subconsciously. The prevent this from occurring, these measurements of the current design need to be validated as inconsequential.
To do this an experiment has been designed in VR where these factors and their various combinations were researched about the perceived distress caused by these measurements
The goal of this experiment is to find the measurements that wont influence people gait.

17.2 Set-up

17.2.1 In reality

the participants were asked to stand in a space of appropriately one meter by one meter to ensure safe use of the VR headset.
The headset used is a Meta Quest 2, used in a standalone modus.

17.2.2 In VR

A table with a button is present. Behind is a virtual model of the current design of the walkway. Around the environment are several props to give a sense of size to the participant. This includes a table with a chair as well as a doorframe.

Image representing the virtual environment from the top

17.3 Method

First, each participant's age and height were recorded, along with any self-reported fear of heights aswell if they had any prior experience with VR. Participants were then asked to put on the VR headset to familiarize with the set-up.
The participants explored the virtual environment and practised using the movement controls, including teleporting, turning, and grabbing virtual objects (such as cubes). These tasks helped participants get comfortable in VR and feel more immersed in the virtual world.
When participants indicated that they were familiar and comfortable in the VR space, the next phase began. They were guided to a VR table which had a button as well as the first variant of the platform design. Participants were asked to teleport on top of the platform as well as to its side to and asked to touch it. This was done to show the difference between their body height and the height of the walkway.
After them experiencing the dimensions of the walkway, they teleported onto it. When on top of the walkway they had to read out aloud the name of the variant. This was done for notation purposes. Afterwards they had to rate how distressed they felt on top of this variant of the walkway. The rating scale was from 0 to 7, where 0 was "no discomfort at all" and 7 was "the scariest thing in their life. After which they were instructed to teleport to the button, to press it and a new random variant would appear. This process was repeated until all variants were tested. While giving their ratings they were encourage to provide additional reasoning for the given score.

17.4 Result

A Repeated Measures ANOVA was done to analyse the effects of Height, Width, and their interaction (Height × Width) on the dependent variable. The results can be seen in the Table 11 below.

Table 11 - ANOVA Results

Measure	F Value	Num DF	Den DF	Pr > F
Height	21.1739	3.0000	21.0000	0
Width	52.3848	3.0000	21.0000	0
Height*Width	5.5661	9.0000	63.0000	0

The main effect of Height was significant(3,21)=21.17, $p<0.001$, indicating that different levels of Height were associated with significant differences in the dependent variable. This suggests that changes in Height alone affected the outcome.
The main effect of Width was also significant, $F(3,21)=52.38$, $p<0.001$, meaning that variations in Width levels also led to substantial changes in the dependent variable. The F value for Width (52.38) was higher than that for Height (21.17), suggesting that Width may have a larger impact on the outcome.
In addition, there was a statistically significant interaction effect between Height and Width, $F(9,63)=5.57$, $p<0.001$. This interaction means that the effect of Height on the outcome depends on the level of Width, and vice versa.
For example, the way the outcome changes with different Heights is not the same at all Width levels. This suggests that Height and Width influence the dependent variable in a connected way, rather than independently.

In Figure 33, these interaction effects can be observed between the various combinations. This graph shows the changes in the mean value of the perceived discomfort

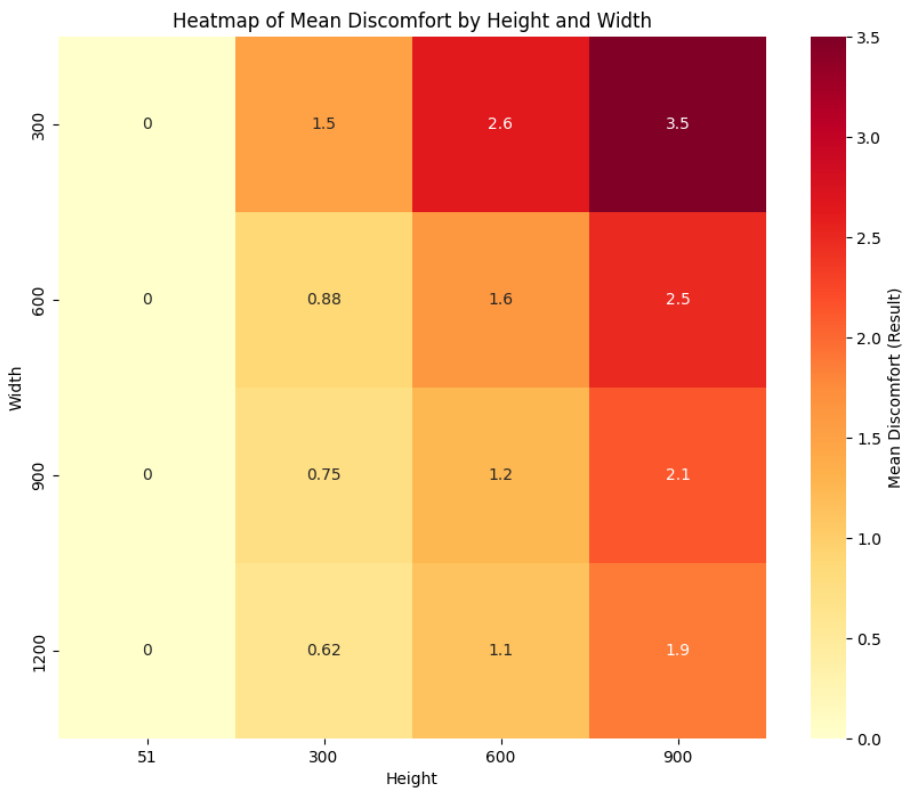

Figure 33 - Heatmap of Mean discomfort by Height and Width

17.5 Discussion

During the experiment, several observations were made. All participants rated the ground-level platform as 0, with some also rating the first level of elevated platforms as 0. However, there was a interesting difference in the rating process. For the ground platform, participants consistently rated it 0 without having teleported on top of it and with minimal decision time. Contrary, for platforms at heights of 300 and above, participants chose to stand on the platform and took several seconds to come to a score. A potential explanation for this is that height influences the score even more than found in this experiment. Additionally, due to time and technology constraints, foot tracking was not done for the VR experiment. Missing the visibility of their feet may have influenced how immersed the participants were, and thus influencing the score they have given.
This notion was further supported by letting participants stand on tables with roughly similiar measurements as the ones in VR and the participants all rated this experience significantly more distressing than the VR experiment.

17.6 Conclusion

The experiment proved that the dimensions of the platform have a significant effect on the perceived discomfort of the patients. This can affect the gait of the patient subconsciously. To prevent this from happening a design that is flat with the floor is needed.
If this isnt an option a design with a wider width and low to the floor is preferred.

18 Appendix: Scanner general comparison

A general comparison between the scanners and thei highest quality modes.

Table 12 - Scanner comparison

	RealSense D435 (current scanner) (Intel, 2026)	Azure Kinect (deprecated)	Femto Bolt (Orbbec Inc, 2023)
Technology	Active IR Stereo Vision	ToF	ToF
Maximum Resolution	1280 x 720	1024 x1024 (unbinned WFOV)	1024 x1024 (unbinned WFOV)
Possible Framerates at the mentioned resolution	6, 15, 30	0,15,15 (unbinned WFOV)	5, 15, (unbinned WFOV)
Focal Distance at the mentioned resolution	28 cm	25 cm (unbinned WFOV)	25 cm (unbinned WFOV)
FOV at the mentioned resolution	87° x 58°	120 x120 (unbinned Wfov)	120 x120 (unbinned Wfov)
Synchronization	Star pattern or daisy chain by the use of diy cable and a diy trigger system which makes it complex	By the use of 3,5 mm jack or software, additional accessories	Star pattern or daisy chain by the use of speciality cable supplied by Orbecc cable or the orbecc sync pro hub can be used
Interference	Yes they interfere but is beneficial for the quality of the scan	Yes, unbeneficial the scans need to happen staggered which causes delay in capturing of the data by 160 us	Yes, unbeneficial the scans need to happen staggered which causes delay in capturing of the data by 160 us
Cost	400	899	528

19 Appendix Comparison overview connectors for the walkway frame

As calculated in Chapter 11.1.5, the primary purpose of the frame-to-frame connectors is to maintain the structural integrity of the flat platform against horizontal braking forces. These frame-to-frame connectors must be able to safely resist the horizontal shear forces and provide sufficient corner rigidity to maintain the structural integrity of the frame under the 400 N lateral load and applied moment of 100 Nm. In the tables below, the structural capacities of several off-the-shelf components are compared against these specific horizontal requirements. A red cell indicates a structural failure, whereas green indicates successful resistance.

Table 13 - Specifications: Connectors used for the frame (Images from (Rexroth, 2019))

	Cube Connector	Bracket (45x45)	Bracket (45x90)	Bracket (45x180)	T-joint
	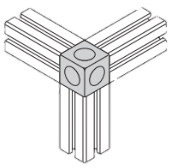	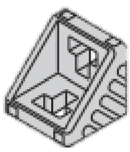	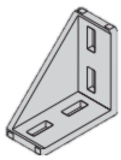	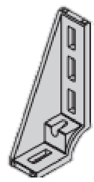	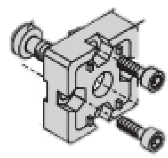
Shear force	-	3000 N	6000 N	3000 N	9000 N
Moment compression	120 Nm	60 Nm	180 Nm	250 Nm	200 Nm
Moment Pulling	120 Nm	160 Nm	400 Nm	-	200 Nm
Torsion	-	-	60 Nm	-	-
Price	6,50	2,10	4,80	12,86	2,95

In Table 14, depicted below, it has been visualized if the forces can be resisted. Red indicates failures, while green indicates success.

Table 14 - Failure check for the given conditions with the frame

	Cube Connector	Bracket (45x45)	Bracket (45x90)	Bracket (45x180)	T-joint
Shortside Moment forwards Inward					
Shortside Moment forward outward					
Longside Moment forwards Inward					
Longside Moment forward outward					

20 Appendix: Comparison overview connectors for the legs to the frame

The connector specifications in the tables below are evaluated against the worst-case peak vertical loads calculated in Chapter 11.2.1 for the leg-to-frame assembly (Concept A). Specifically, to safely mount the legs to the side of the modular frame under a dynamic 5200 N vertical load, the brackets must be able to withstand a maximum vertical shear force of 2600 N, combined with a peak vertical bending moments of up to 650 Nm (long side) and 331.5 Nm (short side). A red cell indicates that a connector fails to meet these extreme structural requirements, whereas green indicates successful resistance.

Table 15 - Specifications: Connectors used for connecting the frame to the legs (Images from (Rexroth, 2019))

	Cube Connector	Bracket (45x45)	Bracket (45x90)	Bracket (45x180)	T-joint	Bracket (90x90)
	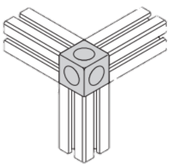	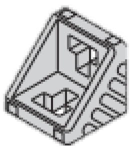	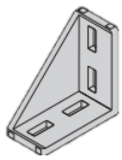	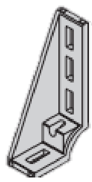	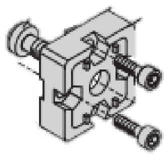	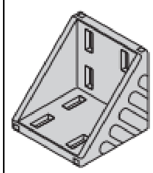
Shear force	-	3000 N	6000 N	3000 N	9000 N	12000 N
Moment compression	120 Nm	60 Nm	180 Nm	250 Nm	200 Nm	370 Nm
Moment Pulling	120 Nm	160 Nm	400 Nm	-	200 Nm	800 Nm
Torsion	-	-	60 Nm	-	-	200 Nm

The connector specifications are evaluated against the worst-case vertical peak loads calculated in Chapter 11.2.1: a vertical shear force of 2600 N and peak vertical bending moments of 650 Nm(long side). A red colour indicates a structural fail, whereas green indicates successful resistance. The results can be seen in Table 15.

Table 16 Failure check for connectors for the given conditions with the legs

	Cube Connector	Bracket (45x45)	Bracket (45x90)	Bracket (45x180)	T-joint	Bracket (90x90)
Shear Force Downward					Not applicable	
long side Moment downwards						

21 Appendix Cost analysis inter frame connectors

Table 17 - Comparison between connectors for the legs of the walkway

	Plate connector 	Bar connector 	Bracket (90x90) 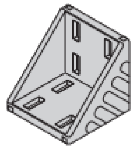
Amount	44	44	44
Individual Price	4,20	7,17	8,50
Total price	184,80	315,48	374

Table 18 - Comparison of prices between concepts for connecting the legs as well as the frame together

Solution	45 Brackets + Plates	45 Brackets + 90 Brackets
Brackets 45x45 (needed) cost	(120) 252,00	(32) 67,20
Brackets 90x90 (needed) cost	-	(44) 374,00
Plates (needed) cost	(44) 180,40	-
Cost total	436,4	441,2

22 Appendix Moment and cost analysis for the connectors that hold scanner assembly

22.1.1 Moment Analysis

In the moment column the final value is determined by adding the weight of the scanner assembly which includes the scanner mount, cheese plate and the femto bolt itself for a total wheight of 1,225 Kg.

Table 19 - Moment calculation caused by the scanner

Camera Naam	Distance (m)	Weight Of the extrusion (kg)	Moment (Nm)	sf	Final Moment (Nm)
Cad2	0,38	0,339	5,87	2	11,73
cad 20	0,23	0,212	3,31		6,6102
cad 21	0,19	0,17	2,58		5,1615
cad 16	0,17	0,127	2,30		4,5968
cad 17	0,24	0,17	3,35		6,696
cad 18	0,39	0,339	6,02		12,0428

As can be seen in the table above a minimal force of 12Nm is applied to the joint.

22.1.2 Specification Joints options analysis

In Table 20 the prices include the connectors and the needed bolts and nuts.

Table 20 - Comparison between connectors to hold the scanner and its support up (Images from (Rexroth, 2019))

Connector	Inner bracket 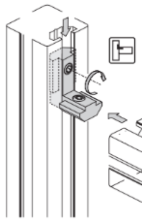	Bracket 3030 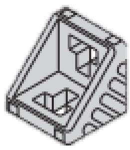	T joint 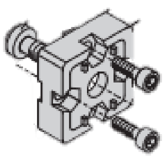
Shear force	600 N	1250 N	4000 N
Moment	10 Nm	25 Nm (75Nm)	80 Nm
Torsion	-	8 Nm	-
Price	1,75	2,65	2,50

23 Appendix: Pixel size calculations for the scanner comparison

	Pixel x	Pixel y	Fov x	Fov y	Plane Size X	Plane Size Y	Pixel Size X	Pixel Size y	Total Area	Distance
Furthest distance										**Distance**
D435										750
	Pixel x	**Pixel y**	**Fov x**	**Fov y**	**Plane Size X**	**Plane Size Y**	**Pixel Size X**	**Pixel Size y**	**Total Area**	
High res	1280	720	87	58	1423,44685	831,4635772	1,112067852	1,1548105	1,284228	
High speed	848	480	87	58	1423,44685	831,4635772	1,678592984	1,7322158	2,907685	
Femto Bolt										
	Pixel x	**Pixel y**	**Fov x**	**Fov y**	**Plane Size X**	**Plane Size Y**	**Pixel Size X**	**Pixel Size y**	**Total Area**	
WFOV Unbinned	1024	1024	120	120	2598,076211	2598,076211	2,5371838	2,5371838	6,437302	
WFOV Binned	512	512	120	120	2598,076211	2598,076211	5,0743676	5,0743676	25,74921	
NFOV Unbinned	640	576	65	75	955,6053912	1150,990482	1,493133424	1,9982474	2,98365	
NFOV Binned	320	288	65	75	955,6053912	1150,990482	2,986266848	3,9964947	11,9346	
Avarage Distance										
D435										**Distance**
	Pixel x	**Pixel y**	**Fov x**	**Fov y**	**Plane Size X**	**Plane Size Y**	**Pixel Size X**	**Pixel Size y**	**Total Area**	500
High res	1280	720	87	58	948,9645667	554,3090515	0,741378568	0,7698737	0,570768	
High speed	848	480	87	58	948,9645667	554,3090515	1,119061989	1,1548105	1,292305	
Femto Bolt										
	Pixel x	**Pixel y**	**Fov x**	**Fov y**	**Plane Size X**	**Plane Size Y**	**Pixel Size X**	**Pixel Size y**	**Total Area**	
WFOV Unbinned	1024	1024	120	120	1732,050808	1732,050808	1,691455867	1,6914559	2,861023	
WFOV Binned	512	512	120	120	1732,050808	1732,050808	3,382911734	3,3829117	11,44409	
NFOV Unbinned	640	576	65	75	637,0702608	767,326988	0,995422283	1,3321649	1,326067	
NFOV Binned	320	288	65	75	637,0702608	767,326988	1,990844565	2,6643298	5,304267	
Bottom Scanner										
Distance at focal length										
D405										**Distance**
	Pixel x	**Pixel y**	**Fov x**	**Fov y**	**Plane Size X**	**Plane Size Y**	**Pixel Size X**	**Pixel Size y**	**Total Area**	70
High res	1280	720	87	58	132,8550393	77,6032672	0,103792999	0,1077823	0,011187	
High speed	848	480	87	58	132,8550393	77,6032672	0,156668678	0,1616735	0,025329	
D405										**Distance**
	Pixel x	**Pixel y**	**Fov x**	**Fov y**	**Plane Size X**	**Plane Size Y**	**Pixel Size X**	**Pixel Size y**	**Total Area**	140
High res	1280	720	87	58	265,7100787	155,2065344	0,207585999	0,2155646	0,044748	
High speed	848	480	87	58	265,7100787	155,2065344	0,313337357	0,3233469	0,101317	
D405										**Distance**
	Pixel x	**Pixel y**	**Fov x**	**Fov y**	**Plane Size X**	**Plane Size Y**	**Pixel Size X**	**Pixel Size y**	**Total Area**	270
High res	1280	720	87	58	512,440866	299,3268878	0,400344427	0,4157318	0,166436	
High speed	848	480	87	58	512,440866	299,3268878	0,604293474	0,6235977	0,376836	

Figure 34 - Pixel size claculations for different scanners, with different resolutions and diffrent distances to the foot.

24 Appendix Cost of the individual frames while in concept

Extrusion type		3030			4545			5050	
lengte	aantal	Price	Total		Price	Total		Price	Total
Big platform									
540	8	5,12	40,96	510	6,82	54,56		13,15	105,2
1000	8	9,49	75,92		13,64	109,12		26,3	210,4
connector	16	1,75	28		2,1	33,6	197,28		
Smaller Platform									
1000	16	9,49	151,84		13,64	218,24		26,3	420,8
140	16	1,33	21,28	110	1,36	21,76		3,682	58,912
connector	32	1,75	56		2,1	67,2	307,2		
Smallest plaform									
600	4	5,69	22,76		8,18	32,72		15,78	63,12
140	4	1,33	5,32	110	1,36	5,44		3,682	14,728
connector	8	1,75	14		2,1	16,8	54,96		
Scan platform									
600	2	5,69	11,38		8,18	16,36		15,78	31,56
540	2	5,12	10,24	510	6,82	13,64		13,15	26,3
connector	4	1,75	7		2,1	8,4	38,4		
			444,7			597,84			931,02

Figure 35 - Concept cost for each variant of the frames while using different extrusion sizes.

25 Appendix Project brief

Designing a 4d foot scanner for research purpose

project title

Please state the title of your graduation project (above) and the start date and end date (below). Keep the title compact and simple. Do not use abbreviations. The remainder of this document allows you to define and clarify your graduation project.

start date 16 - 11 - 2021 25 - 04 - 2022 end date

INTRODUCTION **

Please describe, the context of your project, and address the main stakeholders (interests) within this context in a concise yet complete manner. Who are involved, what do they value and how do they currently operate within the given context? What are the main opportunities and limitations you are currently aware of (cultural- and social norms, resources (time, money,...), technology, ...).

Currently, in personalized footwear design, the design of a shoe or pediatric support is based on a plaster imprint although slowly modern techniques like 3d scanning are being adopted. However, these techniques can only capture a static situation whereas, in real life, a person walks which causes the foot to deform during their step.
To further understand this deformation a scanner is needed that can capture these deformations throughout the gait.
Such a device could help with further refining shoes or pediatrics supports we are currently used to.

Scanners which can accurately capture this kind of data are available for commercial use but are not viable due to their price (€5.000 - €30.000) which in result hampers accessibility for a normal pediatrics office
That was why in a previous graduation project (Vidmar, 2020 & Kwa, 2021) the focus was on designing and prototyping a cheaper 4d scanner that allowed more people access to such a machine, be it pediatrics or research.

However, during this project, the focus will be on designing a machine for researchers. Both can benefit from such a device but the needs and requirements vary a bit between these fields.
Researchers have more benefit from a more flexible device that can be tweaked where they see fit. Be it in hardware, software, or the embodiment of the structure.
For pediatrics, a more out-of-the-box product is needed that can easily be run and clearly defined.

This design consisted of 7 IntelSense D435i cameras that could capture data at 30 fps with a resolution of 848 by 480.
In this design, additional cameras can be added to increase the number of angles the foot is seen from. All the current interactions are done through CLI.
Currently, the person to be scanned has to walk over a raised platform so the bottom of the feet can be scanned by a camera. The platform had to be raised since the depth camera needs a certain depth to function.
However, at the end of the project, several areas of improvement were provided by the author and found by taking a closer look.

space available for images / figures on next page

introduction (continued): space for images

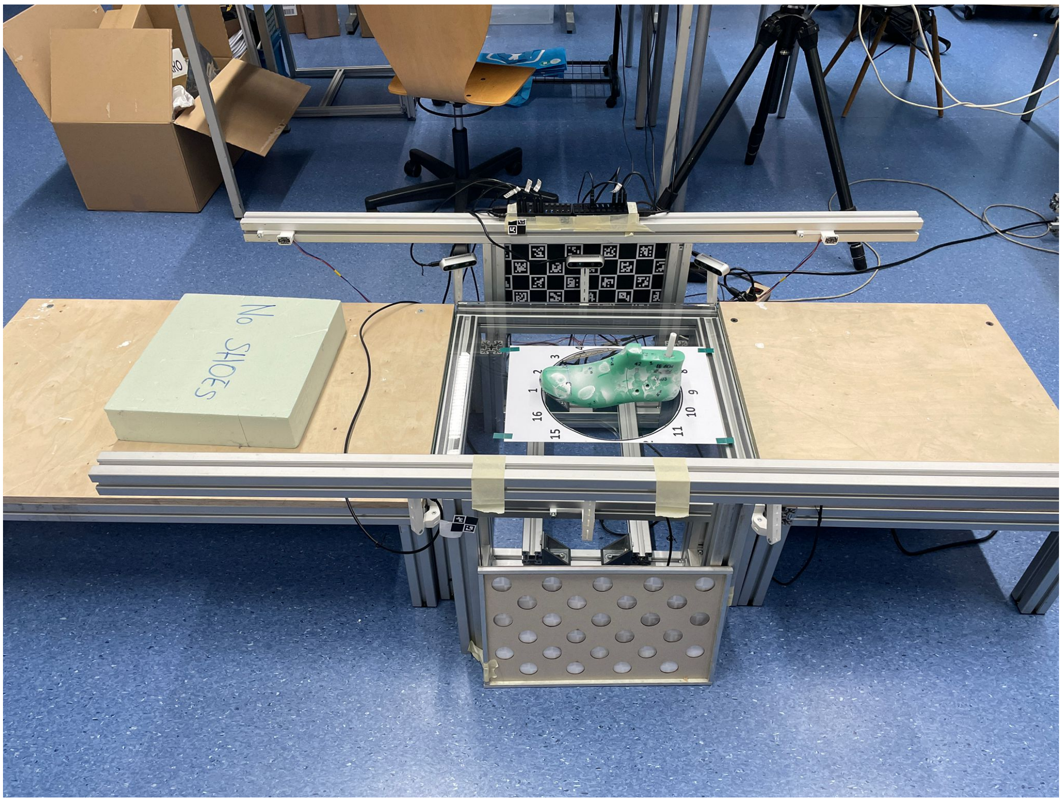

image / figure 1: Current design prototype (side view)

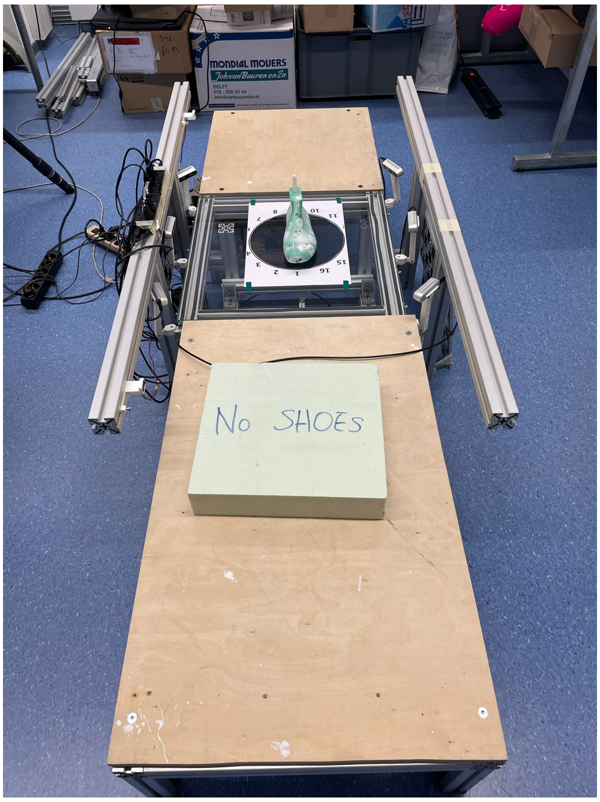

image / figure 2: Current design prototype (front view)

PROBLEM DEFINITION **

Limit and define the scope and solution space of your project to one that is manageable within one Master Graduation Project of 30 EC (= 20 full time weeks or 100 working days) and clearly indicate what issue(s) should be addressed in this project.

The current version of the machine (Kwa, 2021) is a great improvement in comparison to the older version (Vidmar, 2020). But like mentioned before there are several areas that can be improved.

The embodiment of the structure is overengineered, not easily accessible for people with disabilities due to the height, and is not suited for transportation. Redesigning the frame allows for addressing these problems.
The cameras also connect directly to the catwalk which could influence the accuracy which could be solved by decoupling this.
Due to limitations of the hardware and software, the data acquisition loses frames and the subject of scanning has to reduce his/her walking speed which influences the practical use of the scan.
A deeper look into the code with the assistance of Song could lead to significant gains in software by the use of multithreading or using the GPU for computation. For hardware could be looked into researching and acquiring a better setup that has more USB ports, better ram, memory, and CPU.

Lighting conditions influence scan as well, the wrong lighting creates mirror images in the plane where the glass is. This could also be addressed in the camera choice and/or frame design.

Interaction with the machine is all done in CLI which is less accessible and insightful than a GUI. A GUI could increase the ease of use for researchers and pediatrics.
Researching the working order of researchers could allow for a better-designed user interface.

ASSIGNMENT **

State in 2 or 3 sentences what you are going to research, design, create and / or generate, that will solve (part of) the issue(s) pointed out in "problem definition". Then illustrate this assignment by indicating what kind of solution you expect and / or aim to deliver, for instance: a product, a product-service combination, a strategy illustrated through product or product-service combination ideas, ... In case of a Specialisation and/or Annotation, make sure the assignment reflects this/these.

The aim of this project is to improve the current design of the 4d scanner in regards to, embodiment, technique, transportation set-up and use.

For the final deliverable will be a new design of the 4d scanner where it will have:
An optimized modulair frame design with a better camera mount/positioning.
A solution for the mirror images caused by wrong lighting
A better interaction with the machine during transport, set up and use. This includes the interface, the filing structure and data mangement

PLANNING AND APPROACH **

Include a Gantt Chart (replace the example below - more examples can be found in Manual 2) that shows the different phases of your project, deliverables you have in mind, meetings, and how you plan to spend your time. Please note that all activities should fit within the given net time of 30 EC = 20 full time weeks or 100 working days, and your planning should include a kick-off meeting, mid-term meeting, green light meeting and graduation ceremony. Illustrate your Gantt Chart by, for instance, explaining your approach, and please indicate periods of part-time activities and/or periods of not spending time on your graduation project, if any, for instance because of holidays or parallel activities.

start date 16 - 11 - 2021   25 - 4 - 2022 end date

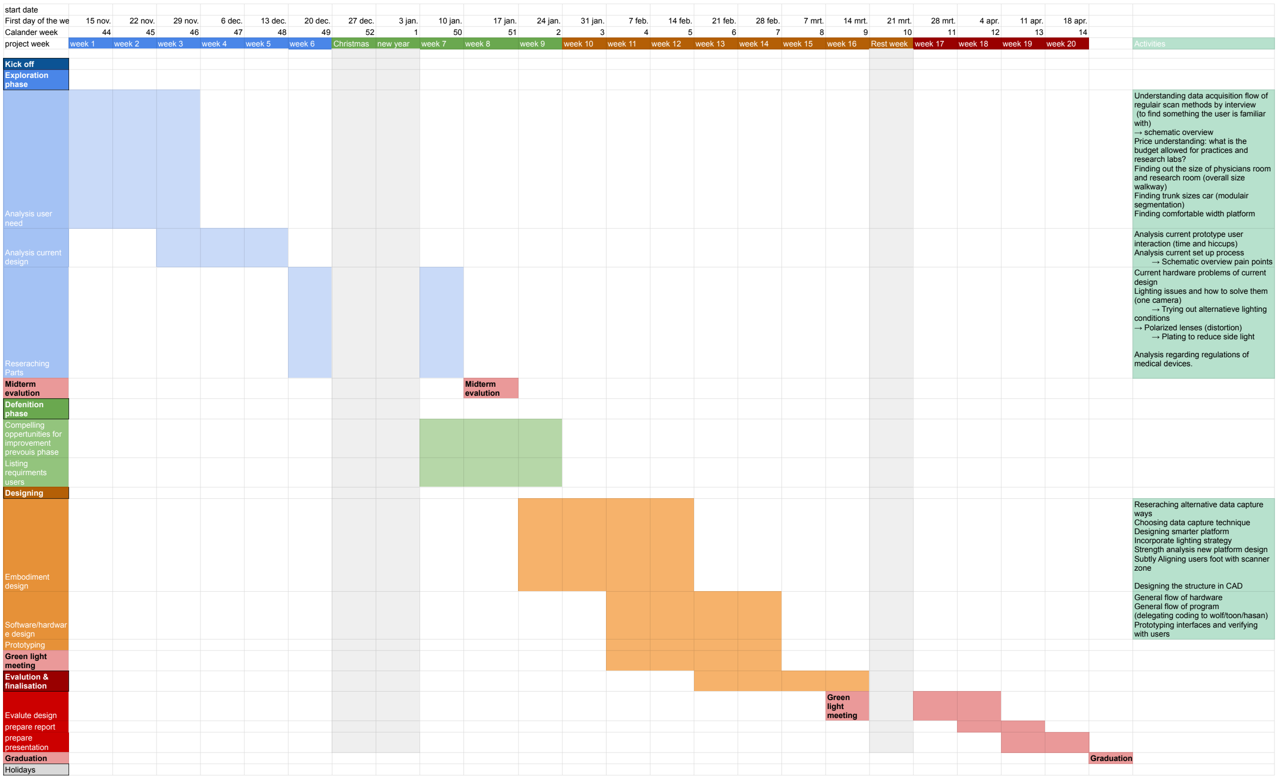

The project will take 23 calendar weeks off which are 3 weeks that are a holiday. 2 weeks of holiday due to the Christmas holiday. This holiday is around week 9 of the project. Another holiday is planned after week 16. This week is for some reflection on the project as well for some rest.

The structure is based on the double diamond method. The first 6 weeks are focused on researching after which 3 weeks will be spent on defining the opportunities and requirements for the product. The next 7 weeks will be spent on designing the final product. A further 4 weeks will be spent on evaluating the design, finalizing the report, and preparing for the presentation.

Important dates:
Kick off meeting: 16 november
Mid term meeting: 17 januari
Green light meeting: 14 march
Graduation ceremony: ...

holiday:
25 december till 10 januari
21 march till 28 march

MOTIVATION AND PERSONAL AMBITIONS

Explain why you set up this project, what competences you want to prove and learn. For example: acquired competences from your MSc programme, the elective semester, extra-curricular activities (etc.) and point out the competences you have yet developed. Optionally, describe which personal learning ambitions you explicitly want to address in this project, on top of the learning objectives of the Graduation Project, such as: in depth knowledge a on specific subject, broadening your competences or experimenting with a specific tool and/or methodology, ... Stick to no more than five ambitions.

The reason I set up this project was to several facets that I found interesting things like advanced prototyping and programming. These are skills I want to further develop due to my personal interest in them. Also, I feel like understanding programming in a better way makes you a better designer due to the increase of smart products. Understanding the code that drives these products can give interesting insights, define your choices better, or allow for better communication with the people that program your code.

During this graduation project, I want to prove I have the competencies of a proper IPD designer. Prove that I can provide a proper balance between several aspects of a product. This was usually done with a group throughout the master but this is a chance to show I can do this on my own.

Furthermore, throughout the project, I want to make more use of the Dutch design guide. I want to further explore this book and make most of the design techniques written in it my own. I feel certain techniques are underutilized and I feel like I can further my skills as a designer by exploring them and actively applying them.

FINAL COMMENTS

In case your project brief needs final comments, please add any information you think is relevant.